ADA045363

(12)

B. S.

RIDE CHARACTERISTICS OF CATAMARAN SEA LOITER
AIRCRAFT IN A SEAWAY

by

Basil S. Papadales, Jr.

Approved for Public Release: Distribution Unlimited

AVIATION AND SURFACE EFFECTS DEPARTMENT



DTNSRDC ASED-384

June 1977



DAVID
W
TAYLOR
NAVAL
SHIP
RESEARCH
AND
DEVELOPMENT
CENTER

UNCLASSIFIED
SECURITY CLASSIFICATION OF THIS PAGE (When Data Entered)

| REPORT DOCUMENTATION PAGE | | READ INSTRUCTIONS BEFORE COMPLETING FORM |
|---|---|---|
| 1. REPORT NUMBER: (14) DTNSRDC/ASED-384 | 2. GOVT ACCESSION NO. | 3. RECIPIENT'S CATALOG NUMBER (9) |
| 4. TITLE (and Subtitle): (6) RIDE CHARACTERISTICS OF CATAMARAN SEA LOITER AIRCRAFT IN A SEAWAY. | | 5. TYPE OF REPORT & PERIOD COVERED: Final Report. |
| | | 6. PERFORMING ORG. REPORT NUMBER |
| 7. AUTHOR(s): (10) Basil S. Papadales, Jr | | 8. CONTRACT OR GRANT NUMBER(s) |
| 9. PERFORMING ORGANIZATION NAME AND ADDRESS: David W. Taylor Naval Ship R&D Center, Bethesda, Maryland 20084 | | 10. PROGRAM ELEMENT, PROJECT, TASK AREA & WORK UNIT NUMBERS: (16) Program Element 63534N, Task Area SSH15002, Work Unit 1612-008 |
| 11. CONTROLLING OFFICE NAME AND ADDRESS: Commander, Naval Air Development Center, Warminster, Pennsylvania 18974 | | 12. REPORT DATE: (11) June 1977 (17) SSH15002 |
| | | 13. NUMBER OF PAGES: 46 |
| 14. MONITORING AGENCY NAME & ADDRESS(if different from Controlling Office): (12) 47p. | | 15. SECURITY CLASS. (of this report): Unclassified |
| | | 15a. DECLASSIFICATION/DOWNGRADING SCHEDULE |

16. DISTRIBUTION STATEMENT (of this Report)

Approved for Public Release: Distribution Unlimited

17. DISTRIBUTION STATEMENT (of the abstract entered in Block 20, if different from Report)



18. SUPPLEMENTARY NOTES

19. KEY WORDS (Continue on reverse side if necessary and identify by block number)

Seaplanes
Sea Loiter Aircraft
Catamarans
Ride Quality

20. ABSTRACT (Continue on reverse side if necessary and identify by block number)

Results from model tests of a catamaran sea loiter aircraft model conducted by The Netherlands Ship Model Basin in 1966 are reviewed. Data are also presented from recent tests of a similar model conducted at the David W. Taylor Naval Ship Research and Development Center. Results from both test programs show that the catamaran hull spacing has little effect on longitudinal motions; lateral motions are strongly affected by hull spacing. The heave and pitch reasonant frequencies are nearly equal.

(Continued on reverse side)

DD FORM 1473, 1 JAN 73 EDITION OF 1 NOV 65 IS OBSOLETE
S/N 0102-014-6601

UNCLASSIFIED
SECURITY CLASSIFICATION OF THIS PAGE (When Data Entered)

387 695

(Block 20 continued)

Hull geometry (other than spacing) and the location of the center of gravity have little effect on motions. The gross size of the aircraft and the various radii of gyration do influence motions. Little damping in roll and pitch is present. Motions of full-scale aircraft are extrapolated from these model results. These scaled data are compared to numerical predictions for similar designs. Heave accelerations at the center of gravity compare favorably; pitch and roll motions do not compare well.

## TABLE OF CONTENTS



## LIST OF FIGURES

LIST OF TABLES

## NOTATION

All dimensions and measurements are presented in U. S. Customary units with International System (SI) units indicated parenthetically. Physical dimensions are described in Figure 1.

| | |
|---|---|
| A | Transfer function |
| B | Hull beam, ft (m) |
| D | Hull spacing, ft (m) |
| $g$ | Acceleration due to gravity, 32.2 ft/s$^2$ (9.80 m/s$^2$) |
| H | Wave height, ft (m) |
| L | Hull length, ft (m) |
| S | Wave half amplitude spectral density, ft$^2$-s (m$^2$-s) |
| $z$ | Heave displacement, ft (m) |
| $\ddot{z}$ | Heave acceleration, ft/s$^2$ (m/s$^2$) or g's |
| $\theta$ | Pitch displacement, rad or deg |
| $\lambda$ | Scale ratio, full-scale/model |
| $\phi$ | Roll displacement, rad or deg |
| $\omega$ | Frequency, rad/s |

Subscripts

| | |
|---|---|
| $z$ | Vehicle in heave |
| $\zeta$ | Wave in heave or slope |
| $\phi$ | Vehicle in roll |
| rms | Root mean square |
| 1/3 | Significant (average of the one-third highest values) |

## ABSTRACT

Results from model tests of a catamaran sea loiter aircraft model conducted by The Netherlands Ship Model Basin in 1966 are reviewed. Data are also presented from recent tests of a similar model conducted at the David W. Taylor Naval Ship Research and Development Center. Results from both test programs show that the catamaran hull spacing has little effect on longitudinal motions; lateral motions are strongly affected by hull spacing. The heave and pitch reasonant frequencies are nearly equal. Hull geometry (other than spacing) and the location of the center of gravity have little effect on motions. The gross size of the aircraft and the various radii of gyration do influence motions. Little damping in roll and pitch is present. Motions of full-scale aircraft are extrapolated from these model results. These scaled data are compared to numerical predictions for similar designs. Heave accelerations at the center of gravity compare favorably; pitch and roll motions do not compare well.

## ADMINISTRATIVE INFORMATION

This investigation was authorized and funded by the Naval Air Development Center under Project SSH15, Program Element 63534N, and Work Unit 1-1612-008.

## INTRODUCTION

Recently, the military potential of an open-ocean sea loiter aircraft has been recognized (Reference 1). Such an aircraft would be capable of taking off and landing in rough water and of loitering afloat in similar sea conditions without exhibiting excessive motions. This routine takeoff and landing capability has been demonstrated with the Shin Meiwa PS-1/SS-2A seaplane. A true open-ocean loiter capability has never been attempted with a flightworthy aircraft.

The design of a sea loiter aircraft is constrained by several demanding requirements, among which are:

- low resistance (in air and water)
- lateral stability while afloat
- high wing and propulsors

* acceptable ride quality (particularly on water)
* adequate reserve buoyancy

The conventional seaplane configuration with a monohull and floats located at the wing tips has satisfied all of these requirements for calm water operations (Figure 2). In rough water (as for a military vehicle) the practicality of this configuration has been challenged, based on the mission-critical nature of a structural failure of a wing tip float; this is a fundamental weakness of the configuration.

Alternative approaches to the general design problem have been suggested. Sponsons (Figure 2) were commonly used on seaplanes prior to World War II. These devices had the advantage of being located near the main fuselage which resulted in an efficient structure. The large volume required to compensate for the short lateral moment arm, however, resulted in large sponsons with high drag and weight. For this reason the use of sponsons diminished as seaplane cruise speeds increased, and smaller wing tip floats became the common alternative.

The use of two large hulls is another suggested approach to the design problem (Figure 2). This configuration, generally called a catamaran, has been employed on only one aircraft, the Savioa-Marchetti S-55. A catamaran aircraft does not suffer from the wing tip failure problem, but this is balanced by increased wetted area and structural inefficiency. The increased wetted area results in increased weight and drag; the torsional loads which must be carried through the structure between the hulls result in a further increase in structural weight. These weight and drag penalities can be reduced by blending this center structure into the two hulls (Figure 2). Reference 2 presents the argument that this configuration would be superior to the conventional seaplane configuration when compared in open-ocean operations where tip float failures would be a serious operational limitation.

In order for the blended catamaran to be applicable to the sea loiter aircraft design problem, the configuration must exhibit acceptable ride quality while floating in rough water. Ride quality is generally measured by heave accelerations and rotational displacements. Although it is generally agreed that these values should be low for good ride comfort, there

is considerable controversy over the quantified limits of acceptability. A summary of this problem is presented in Reference 3.

A review of seakeeping investigations revealed that little experimental or analytical data have been produced concerning catamaran aircraft. This review and estimates of ride quality for two large blended catamaran sea loiter aircraft are presented in this report.

## PREVIOUS TESTS

In 1966 the Netherlands Ship Model Basin (NSMB) conducted a series of seakeeping tests on a small (18.2 lb; 8.26 kg) catamaran seaplane model (Reference 4). A wing and empenage were used to simulate a complete aircraft configuration; details of the model arrangement are shown in Figure 3. The model was designed with two distinct hulls, each similar to a conventional seaplane monohull. Each hull had an L/B of 16.4 with a 60-deg deadrise angle. The distance between the hulls could be varied from D/B = 1.0 to 9.0. Each hull had a beam of 3.94 in. (10.0 cm) which resulted in a beam loading of 4.00. The vertical position of the center of gravity could be varied. Table 1 lists the characteristics of the model as tested.

All tests were conducted in regular waves. Most tests were run with a wave height of 1.57 in. (4.00 cm), although a few selected tests were run at twice this wave height to determine the linearity of the vehicle response. The wave encounter frequency was varied by changing wave length. Heave accelerations at the center of gravity and wing tip were recorded for all tests. Heave, roll, and pitch displacements were also measured. In addition, longitudinal and lateral forces of interest were recorded. All phase lags were noted during the testing. Tests were run at speeds of 0.0, 9.84 ft/s (3.00 m/s), 11.5 ft/s (3.50 m/s), and 13.1 ft/s (4.00 m/s) at headings of 0, 90, 135, and 180 deg. The model hull spacing and height of the center of gravity were varied during the test program. All test results are reported in Reference 4.

The first tests were conducted to determine aircraft natural periods in roll, pitch, and heave; these data are presented in Figure 4. Results from these tests showed that the natural periods in heave and pitch were

nearly equal and independent of the height of the center of gravity and hull spacing. At the larger hull spacings ($D/B \geq 4$), the roll natural period was nearly equal to the values in heave and pitch.

Figure 5 shows the heave and pitch transfer functions in head seas. Both variables were independent of hull spacing and the height of the center of gravity. In pitch, extreme magnification was observed at resonance ($\Delta\theta/\theta_\zeta = 3.7$). The heave resonant frequency was at a similar point (9.0 rad/s), but the magnification was significantly lower ($\Delta z/z_\zeta = 1.45$). At frequencies above 20 rad/s, the heave and pitch responses were negligible. Further tests showed the responses to be linear with wave height.

The effect of hull spacing on heave and roll transfer functions in beam seas is presented in Figure 6. The roll resonant frequency decreased with decreasing hull spacing; the heave resonant frequency increased with decreasing hull spacing. There was no magnification of the heave response at frequencies at or below resonance. Some roll magnification was observed at resonance ($\Delta\phi/0_\zeta = 1.45$).

Test data showed that heave and pitch displacements increased as the heading increased from 90 to 180 deg. All responses were linear with wave height; longitudinal forces (resistance), however, increased at a rate less than linear with wave height. Roll responses were independent of forward speed in beam seas. At all other headings, forward speed resulted in increased motions and heave accelerations. A following seas condition was not tested.

Since all the tests were performed in regular waves, heave acceleration data are of little interest. These data are presented in Reference 4. Results showed that these accelerations were maximized in head seas (at the center of gravity). In beam seas, wing tip accelerations were maximum.

Reference 4 also presents phase lag data for all motions and relative motion data at the wing tips. In general, all motions were in phase with the waves at resonance. Wing tip displacements (in beam seas) were largest at frequencies above the roll resonant frequency.

## TEST PROGRAM

Because of the general lack of knowledge concerning the seakeeping behavior of catamaran seaplane hulls, a model of a conceptual 1,250,000-lb (568,000-kg) blended catamaran sea loiter aircraft design was tested at the David Taylor Naval Ship Research and Development Center (DTNSRDC). Specifically, these tests were conducted in order to gain insight into the ride quality of this type of aircraft in a seaway.

### DESCRIPTION OF MODEL

The test model was specifically designed to simulate a large blended catamaran sea loiter aircraft. The model was tested at a displacement of 640 lb (291 kg), corresponding to a scale ratio of 12.5. The model had a waterline hull length of 11.6 ft (3.53 m) with an L/B of 12.2 and a static beam loading of 5.83. Configuration details of the model are illustrated in Figure 7.

The model hulls were canted outboard at an angle of 22 deg; the inboard side had no warp. The hull step was located 6.32 ft (1.92 m) aft of the forward perpendicular. The forebody was designed with 23 deg of deadrise; the afterbody has no deadrise. The fuselage between the hulls was 0.650 ft (0.198 m) above the static waterline; this structure projected 2.50 ft (0.762 m) ahead of the forward perpendicular. A simulated wing with a span of 19.0 ft (5.79 m) was mounted above the fuselage structure. The wing was 1.40 ft (0.427 m) above the static waterline. The two catamaran hulls could be spaced a distance from D/B = 1.55 to 2.11. The model was ballasted to locate the center of gravity 1.42 ft (0.432 m) above the keel and 5.10 ft (1.55 m) aft of the forward perpendicular. Detail characteristics of the model are presented in Table 2.

### TEST FACILITY

All tests were conducted in the DTNSRDC Maneuvering and Seakeeping (MASK) Facility. This facility measures 360 ft (110 m) by 240 ft (73.2 m) and is 20 ft (6.1 m) deep. Pneumatic wavemakers on adjacent sides of the tank permit generating a wide variety of wave conditions. Regular or irregular wave trains can be generated; irregular waves are generated with programmed spectral characteristics to model scale. The basin is spanned across its length by a bridge which can be rotated to provide

heading changes up to 45 deg from the longitudinal direction. Below this bridge a carriage is suspended from which models are supported. The carriage can move along the bridge to provide model forward speed at different headings; however, this capability was not used for this test program. The carriage was centered above the basin for all tests.

Instrumentation aboard the carriage permits real-time data reduction of model measurements. All data from the model transducers are recorded on strip-chart recorders and stored on magnetic tape for further post-test processing. All testing is video taped.

## TEST PROCEDURE

Initial tests were conducted to measure the natural periods of the model in roll, pitch, and heave. These data were obtained by disturbing the motion (in the mode desired) and by recording the resulting motions. Different hull spacings were used during these tests to observe the effect of changes in the parameter.

A second test series was conducted to determine vehicle response in regular waves. Data from these tests were used to determine vehicle motion transfer functions in head and beam seas. The wave encounter frequency was varied from 1.6 to 6.0 rad/s. During these tests heave accelerations at the center of gravity and cockpit, heave, pitch and roll displacements, and pitch and roll rates were recorded. Further tests were conducted with scaled irregular waves simulating various sea spectra. The characteristics of these test conditions are presented in the appendix. For all of these tests, the model was exposed to head, beam, and following seas.

A final, limited set of tests was conducted with the model exposed to an irregular wave train approaching the bow (head seas) and regular swell approaching from the beam. During these tests the beam sea condition was fixed, and the irregular head seas condition varied. Again, the model hull spacing was varied.

## TEST RESULTS

Results from tests conducted to determine characteristics of the vehicle motion at its natural frequencies are presented in Figure 8.

These data showed that the natural periods in pitch and heave were nearly equal and independent of hull spacing. The natural period in roll was significantly larger than in pitch or heave and was observed to decrease with increasing hull spacing.

The transfer functions of the model in head seas (Figure 9) showed that the model resonated near 2.0 rad/s, and some magnification was observed at this frequency. Motions were damped at higher frequencies. In pitch, the transfer function at resonance was 1.33; the transfer function was 1.15 in heave at the resonant frequency. In beam seas (Figure 10), a magnification of 1.41 in heave was recorded at resonance with some magnification occurring at all frequencies below 4.0 rad/s; no effect of hull spacing was observed. In roll, magnification factors on the order of 7.5 to 10.0 recorded near an encounter frequency of 2.0 rad/s. The roll resonant frequency decreased with decreasing hull spacing.

Figure 11 presents the effect of hull spacing and significant wave height on heave accelerations at the center of gravity and cockpit in head seas. These results showed that these accelerations were independent of hull spacing but increased with increasing wave height. Cockpit accelerations were consistently three times larger than heave accelerations at the center of gravity.

Heave accelerations in beam seas are presented in Figure 12. Test results showed that these accelerations were independent of hull spacing and increased with increasing significant wave height. Cockpit accelerations were 30 to 50 percent higher than accelerations at the center of gravity. Most beam seas data were taken at significant wave heights of 5.0 in. .2 cm) or lower. At higher wave heights the model roll motion became so severe that the test data could not be collected. The magnitude of this problem is shown in Figure 13. This roll displacement data showed that in 5.0-in. (12-cm) significant waves, significant single amplitude roll variations of 10.8 to 12.4 deg were recorded; a 20.1-deg significant roll displacement was recorded at 7.0-in. (18-cm) significant wave height. The magnitude of the roll motions was not dependent upon hull spacing.

Figure 14 presents the heave acceleration data obtained when the model was exposed to a confused sea condition with an irregular wave train approaching the bow and a regular swell approaching the beam. The data showed that increasing the significant wave height of the bow waves resulted in increased heave accelerations at the center of gravity and cockpit. Increasing the hull spacing from D/B = 1.59 to 2.11 resulted in an increase in these accelerations at both locations. Data from the tests conducted with only an irregular wave train approaching the bow are also plotted in Figure 14 for comparison. From this it can be seen that the addition of the beam swell caused no increase in accelerations at the cockpit; the addition, however, did cause a 25- to 50-percent increase in accelerations at the center of gravity.

In general, the severe motions of this vehicle at frequencies at or near resonance resulted in slamming. In head seas, pitch and heave resonance were at frequencies that were nearly equal. Large pitch and heave motions in combination resulted in slamming of the fuselage structure. In beam seas, the large roll motions resulted in the wing tips repeatedly slamming the water at frequencies near roll resonance. Further tests were conducted in following seas, and data recorded from these tests did not differ significantly from the data taken during tests with the model in head seas.

## DISCUSSION

### GENERAL TEST RESULTS

The NSMB and DTNSRDC models displayed similar responses to regular waves in both head and beam seas. In head seas, the hull spacing had no effect on the longitudinal vehicle motions. In beam seas, however, an increase in hull spacing resulted in increased natural frequencies in roll. The DTNSRDC model exhibited little effect of hull spacing on heave motions in beam seas, although the NSMB model was observed to have an increased resonant frequency with lower hull spacings. This difference can be attributed to the differences in fuselage clearance and hull shape of the two models.

The tests also showed that the height of the center of gravity had little effect on motions. The two models displayed different motion amplification in pitch and roll which can primarily be attributed to differences in radii of gyration. The NSMB model had large pitch amplification at resonance which resulted from a proportionately large pitch radius of gyration; the DTNSRDC model had less amplification and a lower radius. In beam seas, the NSMB model had some roll amplification at resonance, and the DTNSRDC model was observed to have very large amplification. This difference was probably due to the DTNSRDC model having a proportionally larger roll radius of gyration than the NSMB model. The NSMB model had roll and heave resonant frequencies which were nearly equal in beam seas (Figure 6); the pitch and heave resonant frequencies were also very close in head seas (Figure 5). The same was true for the DTNSRDC model (Figures 9 and 10). This phenomenon of co-incident resonant frequencies would result in a severe ride (particularly in head seas where the pitch and heave motions can be superimposed).

## SCALED RESULTS

### Method of Scaling

Two independent approaches were used to scale model heave acceleration data to full scale. The more direct method was to Froude-scale the heave acceleration data recorded from the model when subjected to a simulated sea spectra. This method requires a large number of wave encounters to provide an accurate statistical data base. This approach could be used only with the DTNSRDC model, since the test program permitted scaled irregular wave tests. The major disadvantage of this approach is that the direct scaling can only be used to scale the vehicle and wave spectra together; hence data is limited to one sea state for a given full size vehicle. It is possible to conduct a statistical analysis of the wave and response power spectra and to derive a Response Amplitude Operator (RAO) which is applicable for any sea condition represented as a spectra. This approach is described in Reference 5. The complexity of this approach precluded its use in this preliminary analysis.

An alternate approach to scaling heave accelerations was used for both sets of model test data. This indirect method was used to calculate heave accelerations only at the center of gravity. Test results showed that accelerations at this point were the lowest anywhere in the aircraft structure.

This method of scaling was based upon the assumption that the wave spectra and the response spectra could be modeled by the linear superposition of a series of harmonic functions of varying amplitude and frequency. The wave amplitude spectral density is defined by:

$$2S_{\zeta}(\omega)d\omega = z_{\zeta}(\omega)^2 \tag{1}$$

Similarly, the vehicle response spectra (in heave) can be represented by:

$$2S_{z}(\omega)d\omega = z(\omega)^2 \tag{2}$$

This response spectra can be integrated, and this integrated value can be used to characterize the specta; that is,

$$(z_{rms})^2 = \int_0^{\infty} S_z(\omega)d\omega \tag{3}$$

It is interesting to note that this integral is equal to the variance of the power spectra and, therefore, is equal to the mean square value of the statistical base. Generally, the root mean square (rms) is used to characterize the data.

Substituting Equation (2) into this integral equation yields:

$$(z_{rms})^2 = \frac{1}{2}\int_0^{\infty} z(\omega)^2 d\omega \tag{4}$$

The mean square heave acceleration can be computed in a similar manner:

$$(\ddot{z}_{rms})^2 = \frac{1}{2}\int_0^{\infty} \ddot{z}(\omega)^2 d\omega \tag{5}$$

This spectrum can be related to the heave displacement spectrum by use of the assumption that $z(\omega)$ can be represented by the linear superposition of a series of harmonic functions. At any frequency, the heave acceleration can then be calculated from:

$$\ddot{z}(\omega)_{max} d\omega = \omega^2 z(\omega) d\omega \tag{6}$$

Substituting,

$$(\ddot{z}_{rms})^2 = \frac{1}{2}\int_0^\infty \omega^4 z(\omega)^2 d\omega \tag{7}$$

The heave response of the model, $z(\omega)$, can be related to the wave amplitude, $z_\zeta(\omega)$, by a transfer function $A_z(\omega)$ defined by

$$z(\omega) = A_z(\omega) z_\zeta(\omega) \tag{8}$$

Substituting Equation (8) into Equation (7) yields:

$$(\ddot{z}_{rms})^2 = \frac{1}{2}\int_0^\infty \omega^4 A_z(\omega)^2 z_\zeta(\omega)^2 d\omega \tag{9}$$

Scaling of the transfer function $A_z(\omega)$ requires only Froude scaling of the encounter frequency. This indirect method of scaling heave accelerations was employed to obtain full-scale estimates for both the NSMB and DTNSRDC models. A Pierson-Moskowitz model was used to generate the wave power spectra (see the Appendix).

In a similar manner, the roll or pitch motion of the vehicle can be scaled, except that in these cases the displacements rather than accelerations are of primary interest. For large vehicles, pitch motions can add to heave motions, thus making heave motions more severe. This problem is generally overcome by locating the crew near the center of gravity. Roll motions, however, can be discomforting without the addition of any translational motion. Catamaran hulls have been noted to lack roll damping; hence, roll motions are generally included in a discussion of ride quality.

$$(\phi_{rms})^2 = \frac{1}{2}\int_0^\infty \phi(\omega)^2 d\omega \quad (10)$$

In roll, the convention is to quote values in terms of the significant roll rather than the root mean square; this can be calculated by:

$$\phi_{1/3} = 2.00\ \phi_{rms} \quad (11)$$

As with the heave motion, a transfer function can be defined where the motion response of the vehicle is related to the wave motion; that is,

$$\phi(\omega) = A_\phi(\omega)\phi_\zeta(\omega) \quad (12)$$

Substituting into Equations 10 and 11:

$$(\phi_{1/3})^2 = \int_0^\infty A_\phi(\omega)^2 \phi_\zeta(\omega)^2 d\omega \quad (13)$$

The wave slope spectra was computed from a Pierson-Moskowitz spectrum as presented in the Appendix. This method was used to obtain full-scale estimates for both models. As in the case of heave motions, the full-scale motions could be estimated from directly scaled data from irregular wave experiments. This method was used for comparison with the data from the DTNSRDC model.

Estimate of Ride Quality of 1,250,000 Pound (568,000 Kilogram) Aircraft

Test results from both models were used to estimate the heave acceleration of similar aircraft with a displacement of 1,250,000 lb (568,000 kg). The DTNSRDC model was tested in a series of simulated sea spectra scaled for this displacement. Hence, both methods could be directly compared. Indirect scaling, by use of the heave transfer function, was used solely to calculate full-scale accelerations of the NSMB model. Results from these calculations are presented in Figure 15. The heave accelerations increased with significant wave height. The indirect method of obtaining accelerations yielded results approximately 10 percent higher than results from direct scaling of the DTNSRDC model. This was presumably due to difference between test wave spectrum and Pierson-

Moskowitz spectrum (see Appendix). The NSMB model had accelerations approximately 50 percent greater than the DTNSRDC model. This can be attributed to the higher frequency of the NSMB model (full-scale) which resulted in a larger portion of the wave spectra falling near resonance.

References 6 and 7 present the predicted heave accelerations of a similar catamaran aircraft with the same displacement. A comparison of this aircraft with the scaled-up aircraft from the two model test programs is presented in Table 3. Results from the DTNSRDC tests compare favorably with data from these references (Figure 15). Due to the geometric differences between the model and the aircraft used in References 6 and 7, this favorable comparison must be treated as coincidental.

The effect of changing the headings of the models to beam seas is shown in Figure 16. The NSMB model had lower accelerations in beam seas due to the lower resonant frequency in heave (Figures 5 and 6). The DTNSRDC model had higher accelerations because this frequency and amplification at resonance increases in beam seas.

Figure 16 presents the significant roll estimated as a function of significant wave height for the two models in beam seas. In this condition the NSMB design would have substantially lower roll motion. This is primarily due to the much lower roll amplification observed with this model. Differences in resonant frequencies had little effect. Differences in roll characteristics of the two models can be seen by comparing Figures 6 and 10. In all cases, vehicle roll motion increased with the significant wave height, and for both models this motion was quite large, even in calm seas. Comparison of methods of scaling for the DTNSRDC model indicates that the indirect method resulted in roll values approximately 5 percent lower than the directly scaled results.

Estimate of Ride Quality of 640,000 Pound (291,000 Kilogram) Aircraft

Reference 8 presents a design of a 640,000 lb (291,000 kg) blended catamaran sea loiter aircraft. The NSMB and DTNSRDC test results were scaled to this displacement. Table 4 lists the significant characteristics of the full-scale aircraft and of the models scaled to this weight.

Figure 17 presents the heave accelerations at the center of gravity of the various aircraft in head and beam seas. All heave acceleration

trends were identical to those predicted for the 1,250,000 lb (568,000 kg) aircraft. This is due to the nature of the Froude scaling of the data. Predictions (from Reference 8) in head seas were substantially lower than either of the scaled model data. At the lower wave heights, the predicted results were approximately 50 percent lower than the results of the DTNSRDC test data. The data from Reference 8, however, showed a more linear increase in acceleration with significant wave height. Thus, the large difference at the lower wave heights was reduced with increasing wave height. Again, configuration differences between the various aircraft shown in Figure 17 must be considered. The substantial difference in the predicted heave accelerations can be attributed only to differences in hull shape. Differences in accelerations can also be attributed to different sensor locations and pitch radii of gyration.

The effect of increasing significant wave height in beam seas on the roll motion of the various designs is presented in Figure 18. These results are similar to the data presented in Figure 16 for the larger aircraft. Roll displacements, as with accelerations, were larger for the smaller aircraft because of the higher resonant frequencies characteristic of a smaller vehicle. Froude scaling will always yield a higher resonant frequency for a smaller vehicle if the mass and geometric characteristics are also scaled. Because the sea conditions are fixed, the higher resonant frequency (in roll, pitch, or heave) will result in more of the sea spectra causing an undamped vehicle response which results in higher accelerations and larger motions.

## CONCLUSIONS

Results from the NSMB and DTNSRDC catamaran sea loiter aircraft seakeeping tests support the following conclusions:

1. In head seas, the aircraft hull spacing has negligible effect on the pitch and heave motions. Specifically, the resonant frequencies are unaltered.

2. In beam seas, an increase in hull spacing results in an increase in the roll resonant frequency and, perhaps, some decrease in the heave resonant frequency.

3. For hulls of relatively high L/B (10-15), the resonant frequencies in pitch and heave will be approximately equal (although large changes in conventional pitch radii of gyration could alter this). This could result in severe motions at or near this resonant frequency.

4. For hull spacings which are relatively large (D/B > 5), the roll natural frequency is also close to that in heave and pitch. A change in the radii of gyration in either pitch or roll could alter this somewhat. Larger hull spacings could also alleviate this problem.

5. The hull geometry (L/B, beam loading, etc.) has little effect on motions for reasonable geometric shapes.

6. The vertical position of the center of gravity has little effect on motions (within reasonable limits).

7. The effects of the pitch radius of gyration on vehicle motions in head seas is unclear. Experience with monohulls, however, indicates that this parameter should be kept small (on the order of 25 percent of the waterline hull length) for minimal motions. Numerical predictions of catamaran motions (Reference 6) substantiate this, although definitive model tests have not been conducted.

8. The roll radius of gyration has some effect on roll motions, and this characteristic dimension should be kept to a minimum if roll motions are to be minimized. This is suggested from extrapolations of model data (Figures 16 and 18).

9. Motions can be significantly reduced in a given sea condition by a Froude-scaled increase in size and displacement.

10. For full-scale vehicles of the size of interest (640,000 to 1,250,000 lb; 291,000 to 568,000 kg), the resonant frequencies in roll, pitch, and heave will be greater than the frequency of maximum wave energy for moderate and higher sea states ($\omega = 0.7 - 1.0$ rad/s). This would result in motions becoming more severe if the wave encounter frequency were increased by forward motion. This effect has been observed with smaller monohull sea loiter aircraft (Reference 9); motions could also be reduced by decreasing the encounter frequency using forward speed in following seas. This technique should be applicable to the large catamaran aircraft, since both the large aircraft and the smaller monohull

aircraft in Reference 9 have resonant frequencies greater than the wave spectra energy maxima.

11. Heave accelerations at the center of gravity are slightly dependent on heading; accelerations are somewhat lower in head seas. These accelerations (in head seas) are increased by the addition of a beam swell.

12. Cockpit accelerations are minimized in beam seas and maximized in head seas. The addition of a beam swell in head seas reduces the accelerations; however, the mechanism responsible for this phenomenon is not understood.

13. Wing tip accelerations are maximized in beam seas and minimized in head (and following) seas.

14. In general, the catamaran configuration displays little roll and pitch damping. This results in severe motions near resonance at all headings. These large motions, if undamped, require large wing heights and fuselage clearances (for blended catamarans) to avoid slamming.

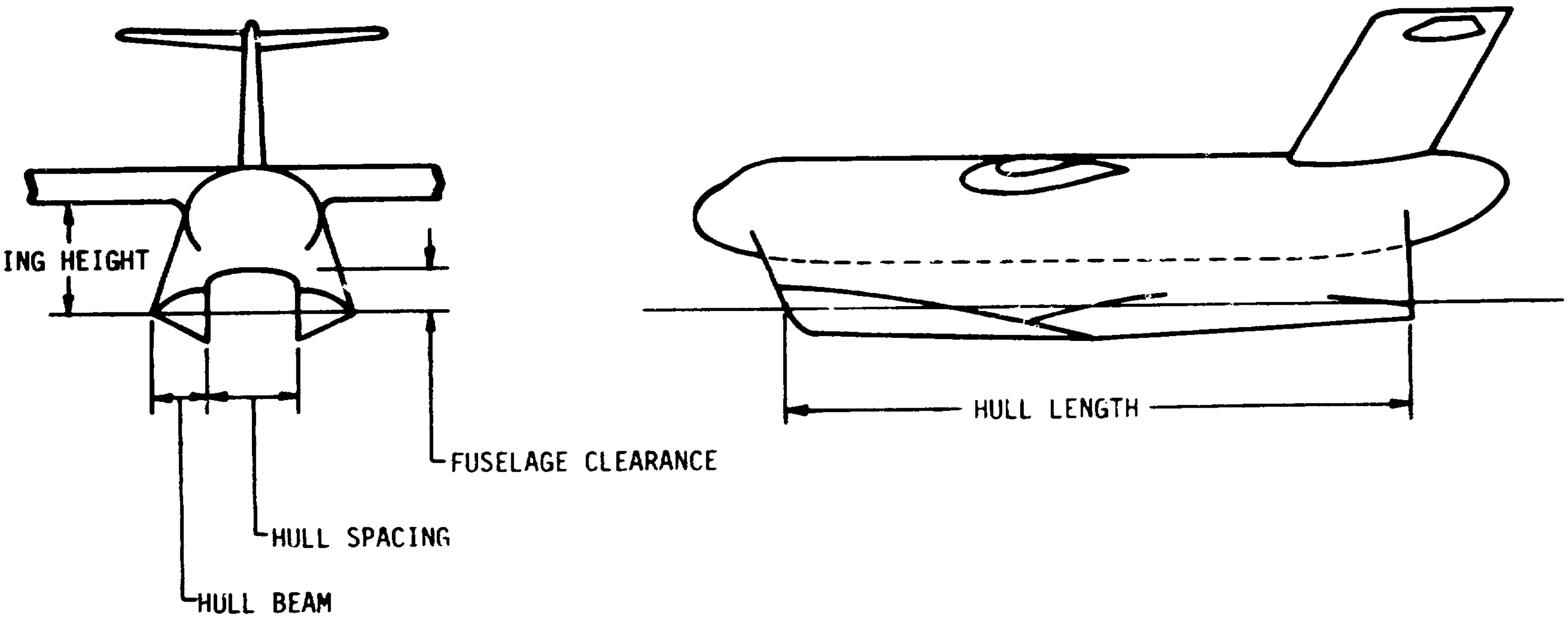


Figure 1 - General Notation

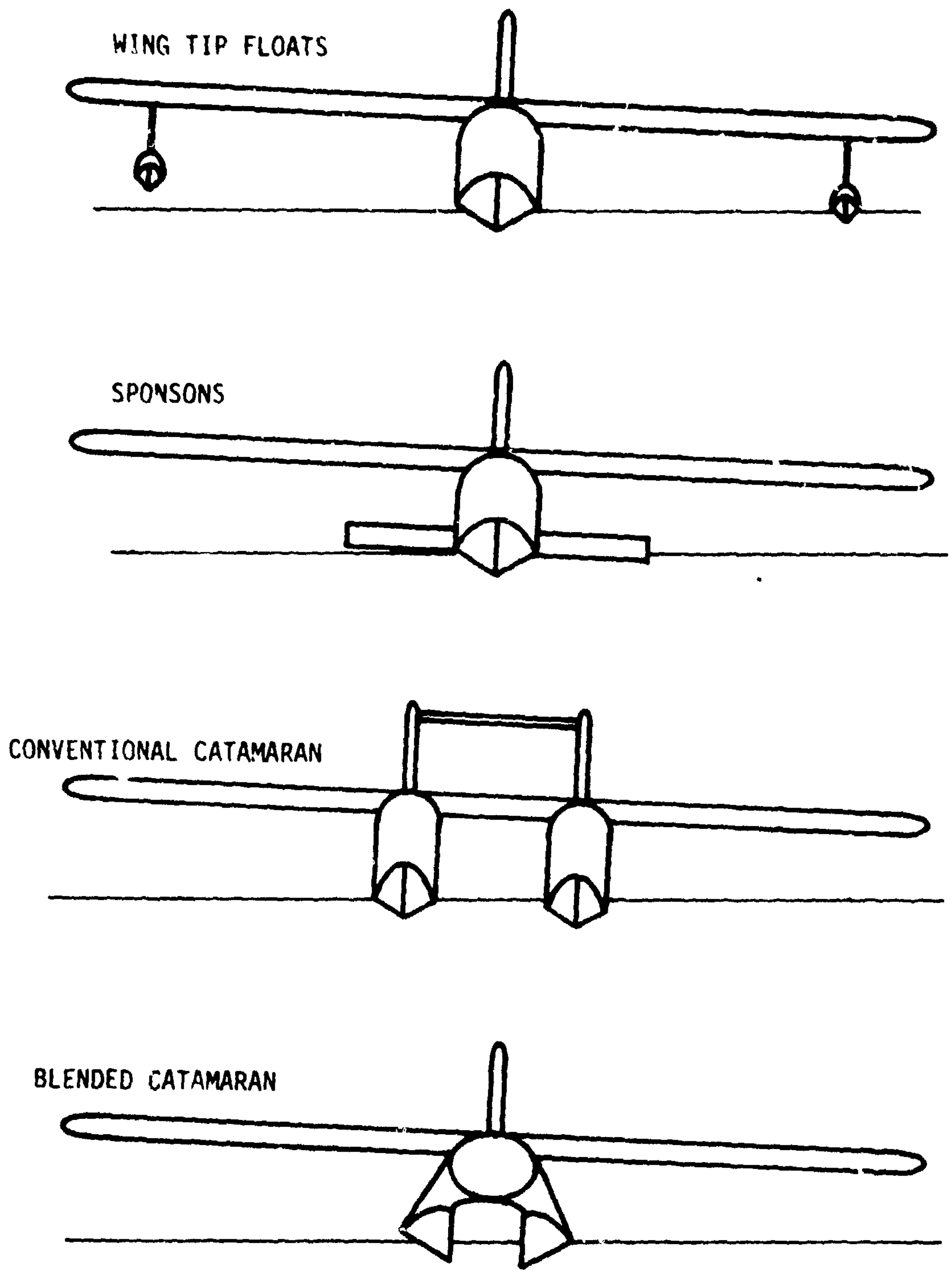


Figure 2 - Lateral Flotation Devices for Seaplanes

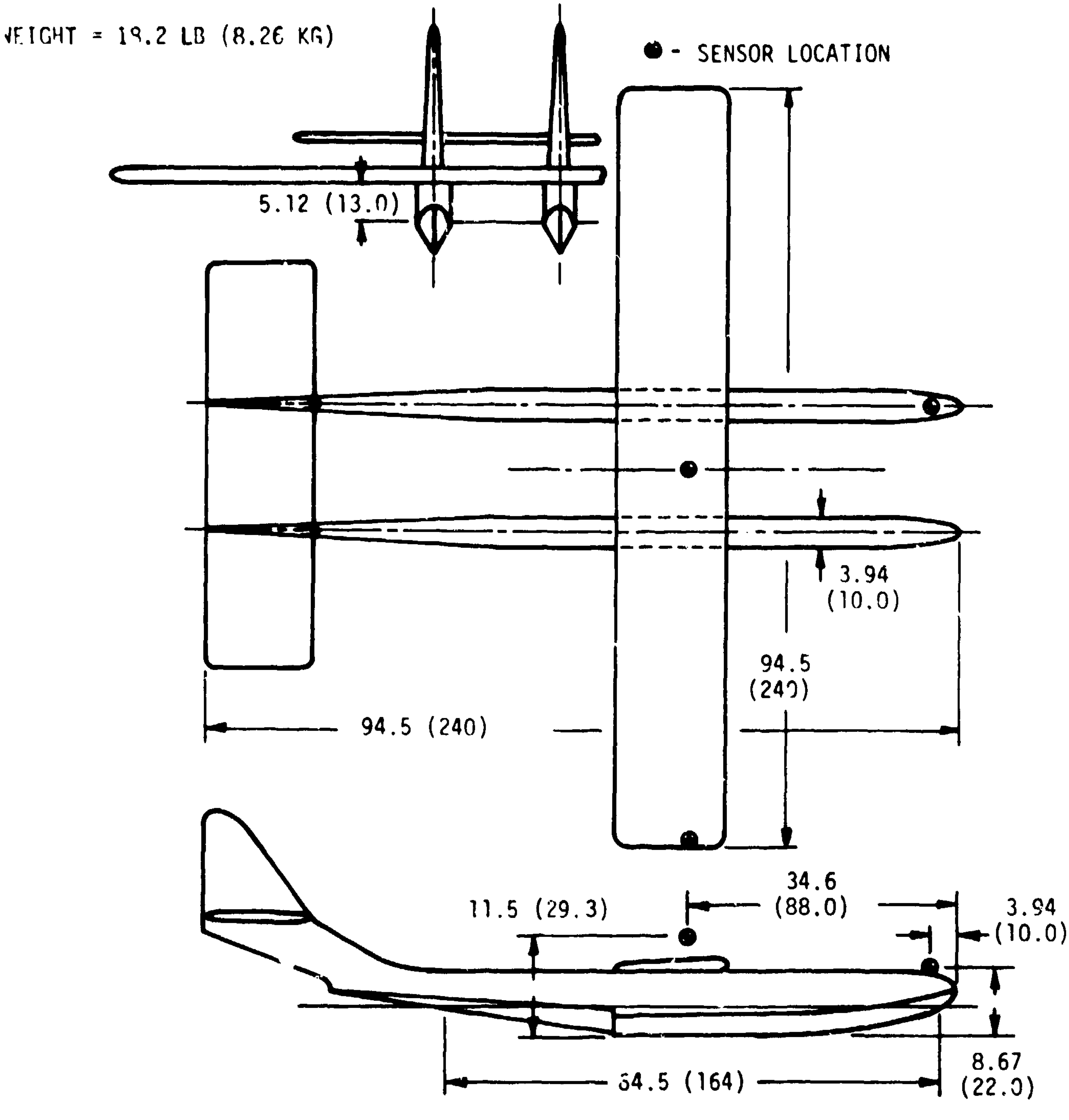


Figure 3 - General Arrangement of NSMB Model

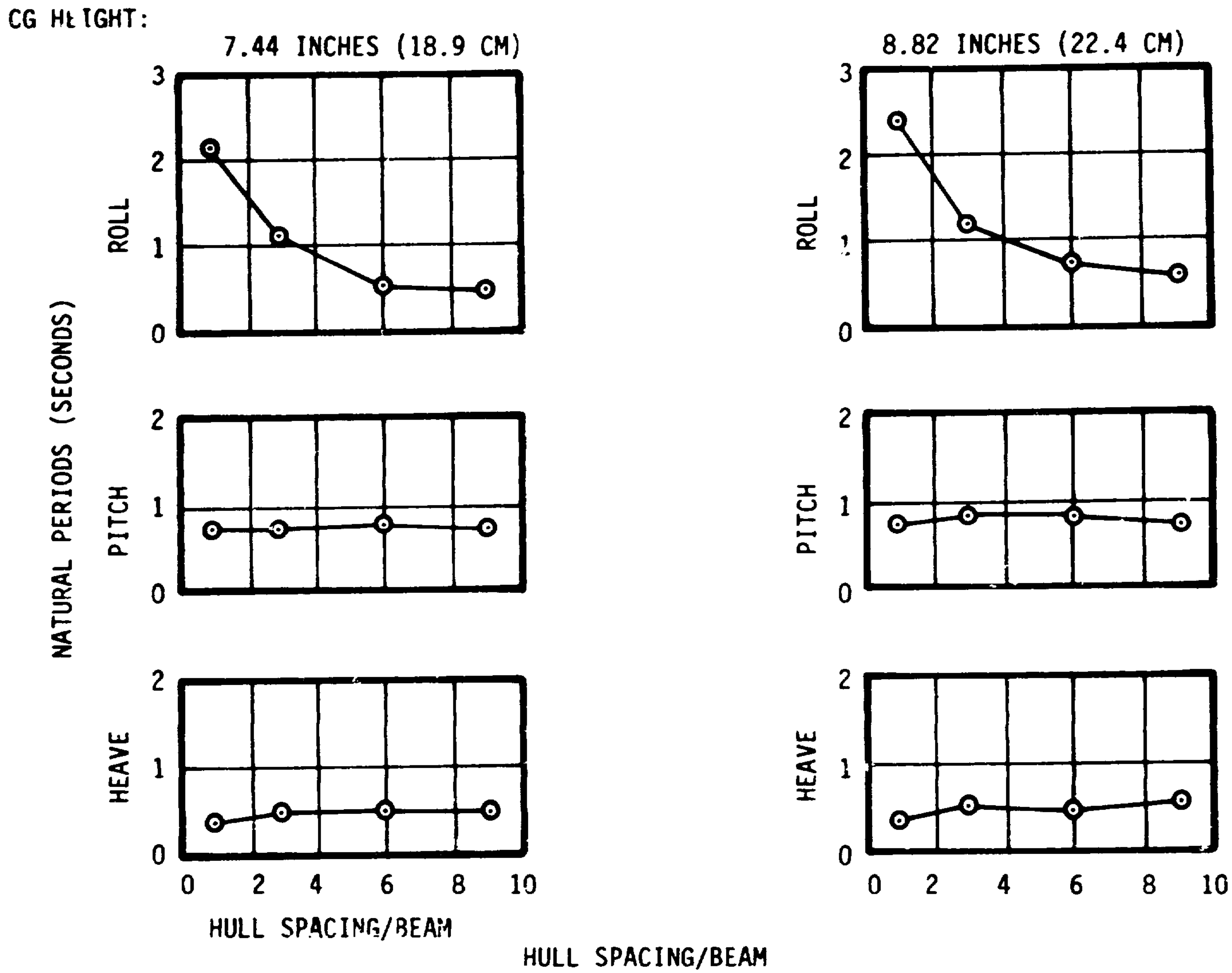


Figure 4 - Natural Periods of NSMB Model

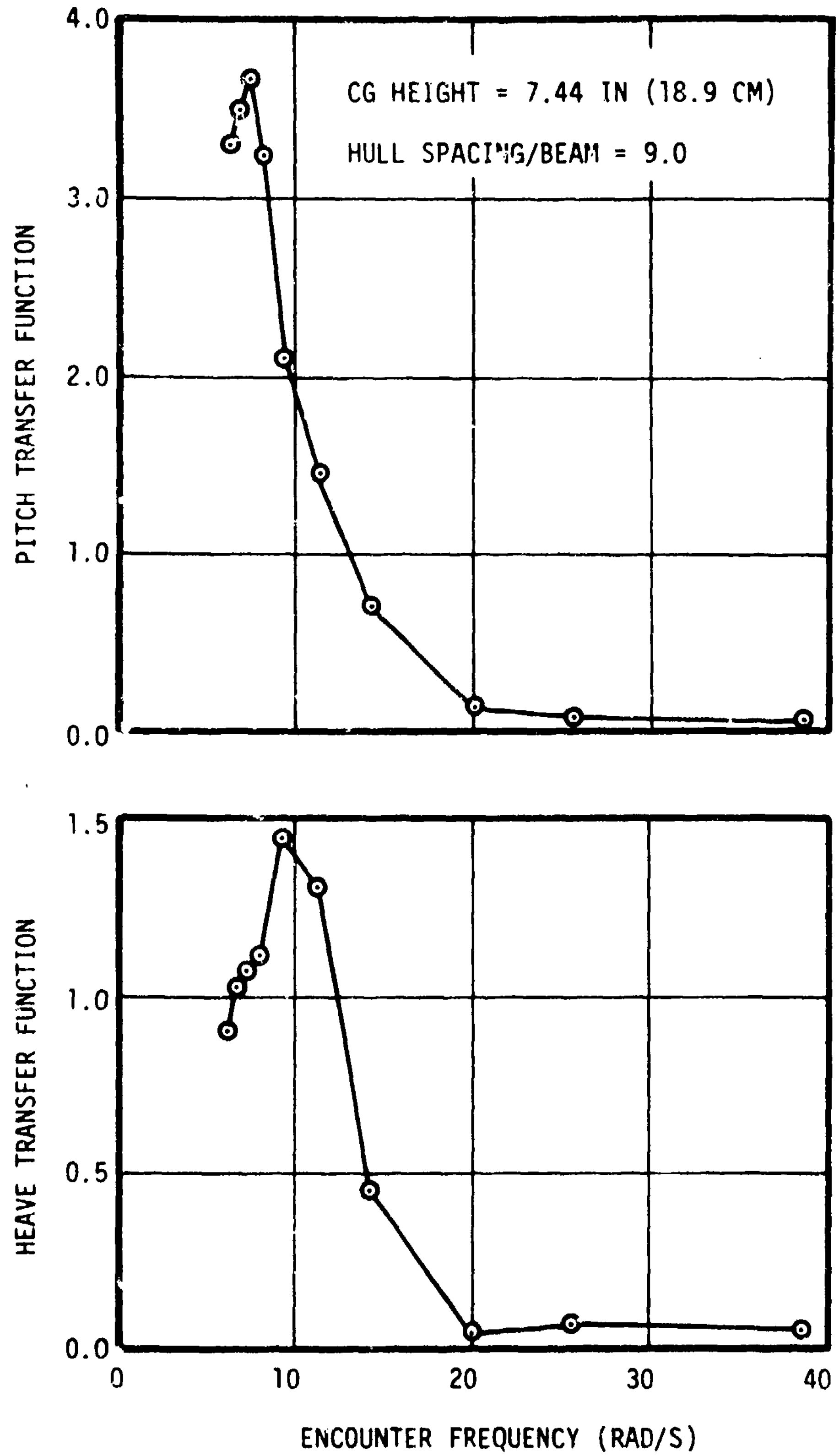


Figure 5 - Transfer Functions of NSMB Model in Head Seas

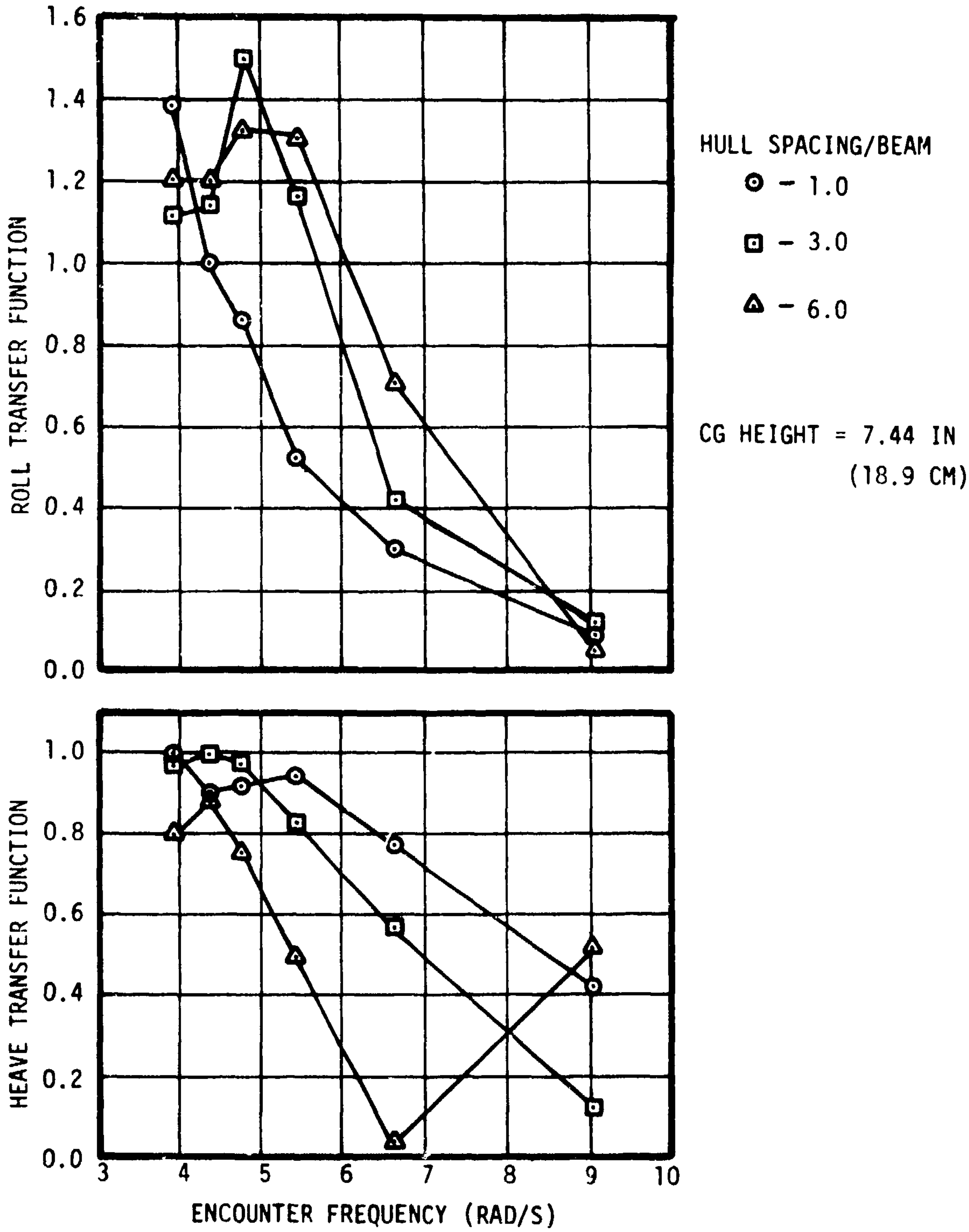


Figure 6 - Transfer Functions of NSMB Model in Beam Seas

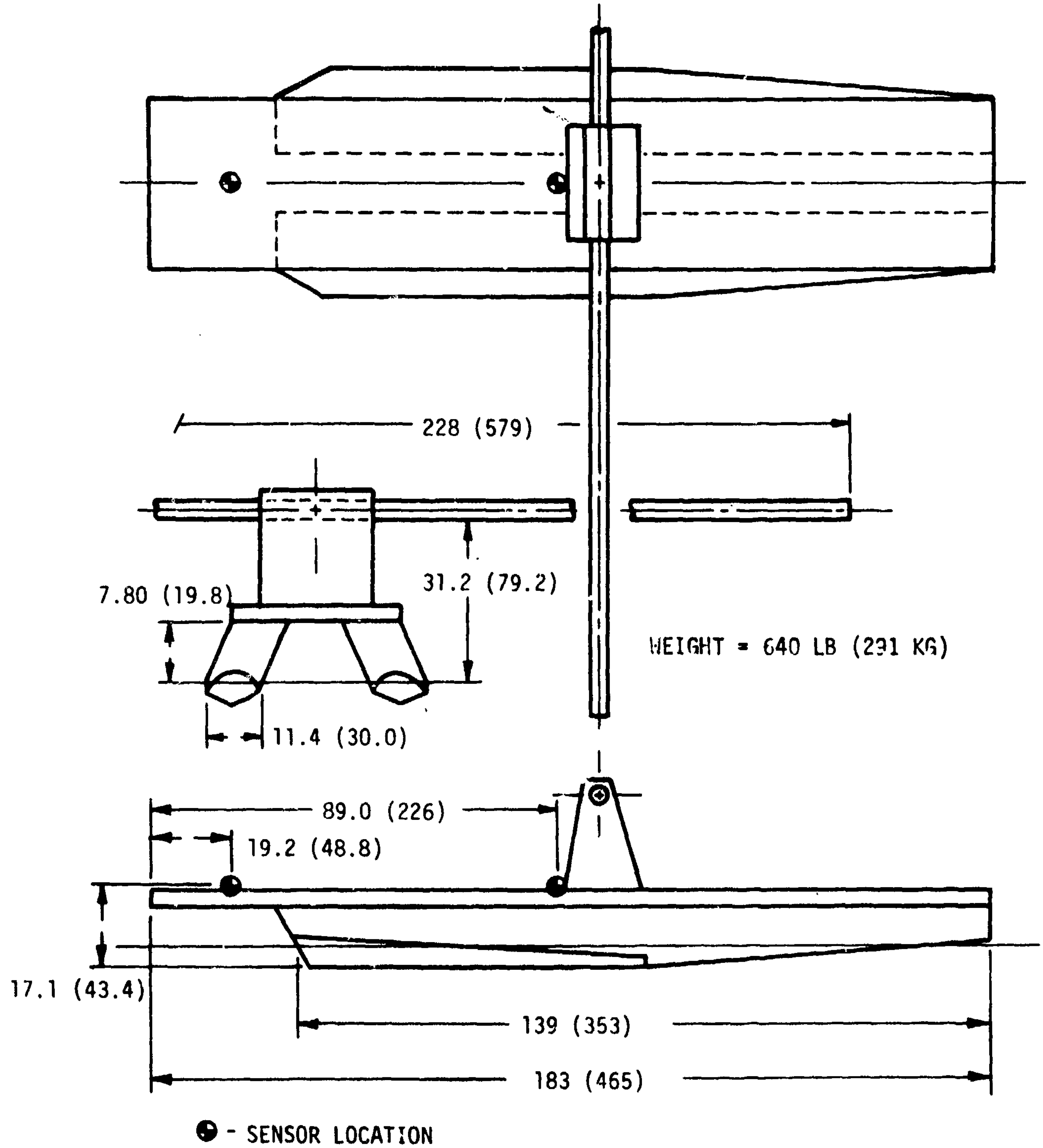


Figure 7 - General Arrangement of DTNSRDC Model

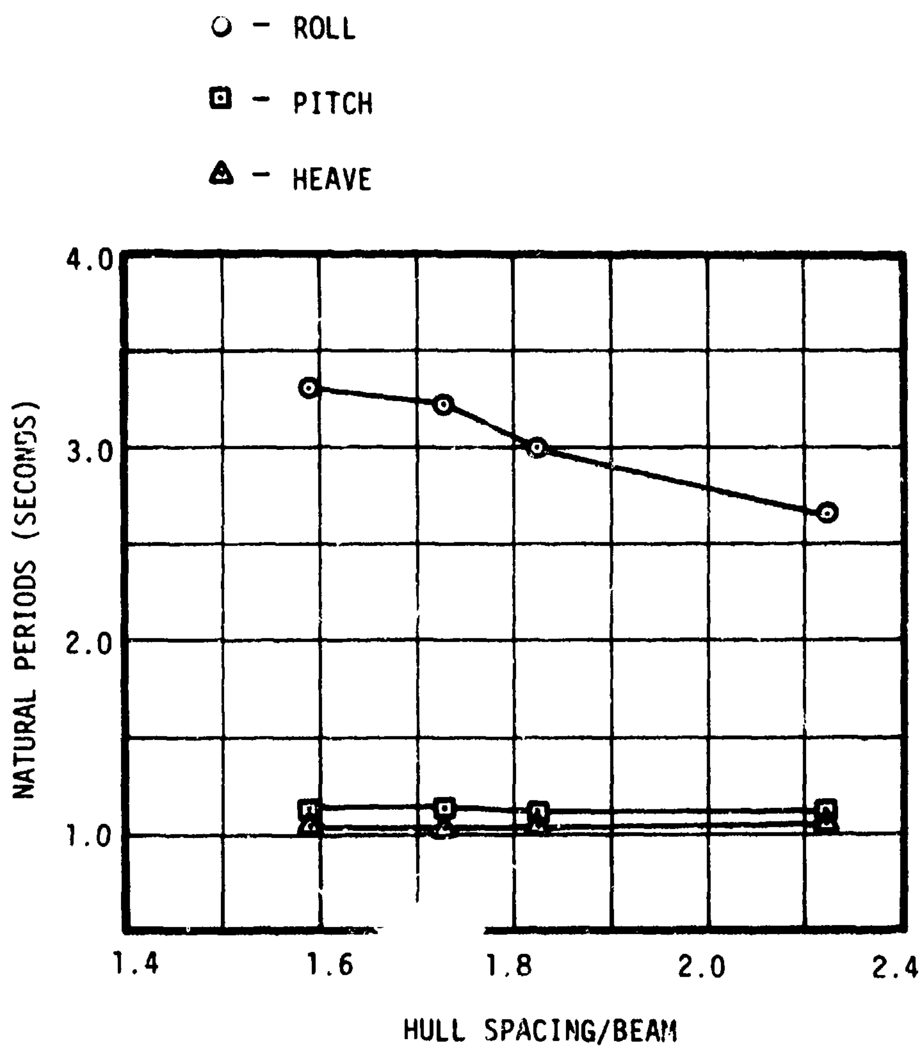


Figure 8 - Natural Periods of DTNSRDC Model

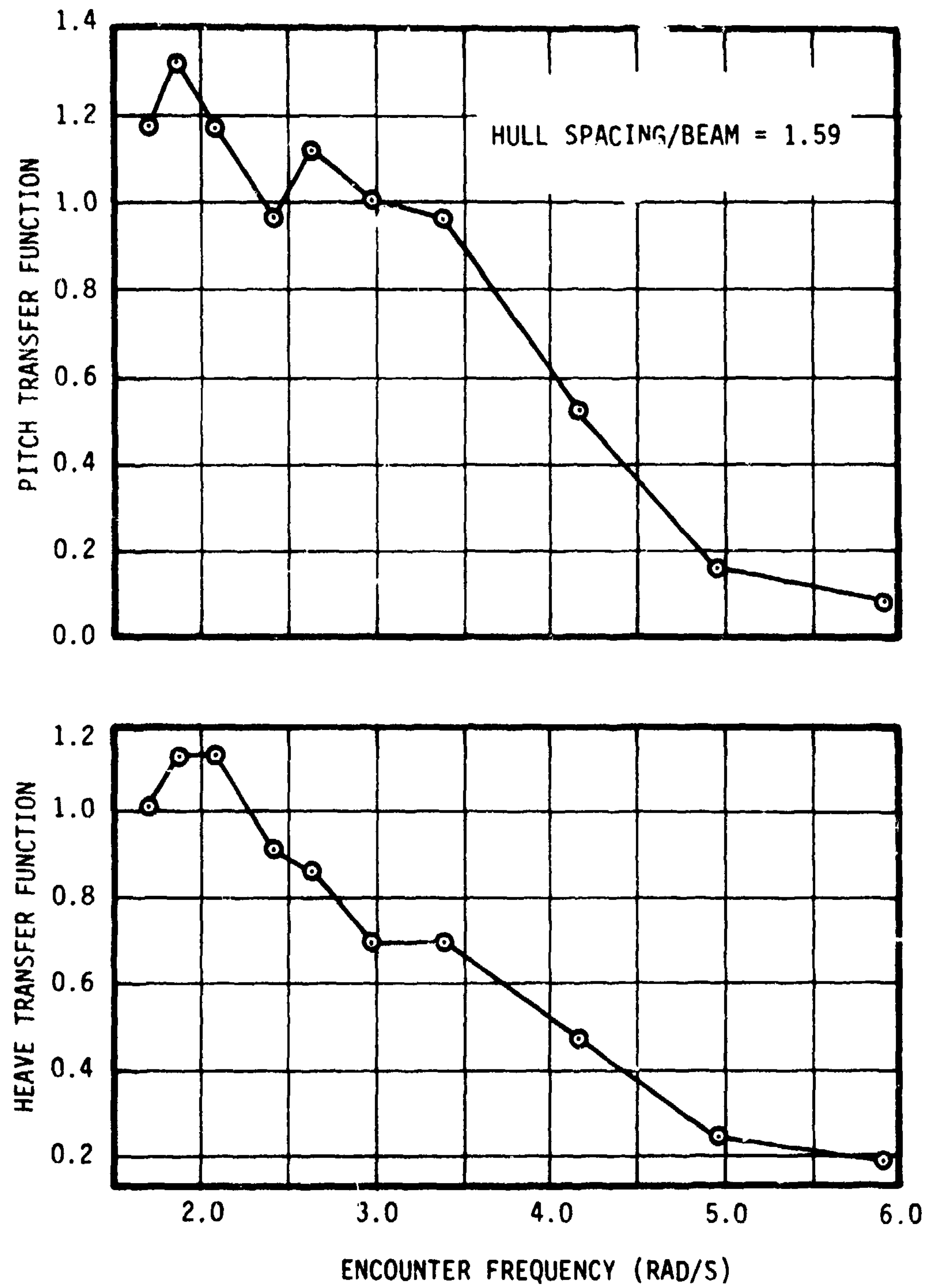


Figure 9 - Transfer Functions of DTNSRDC Model in Head Seas

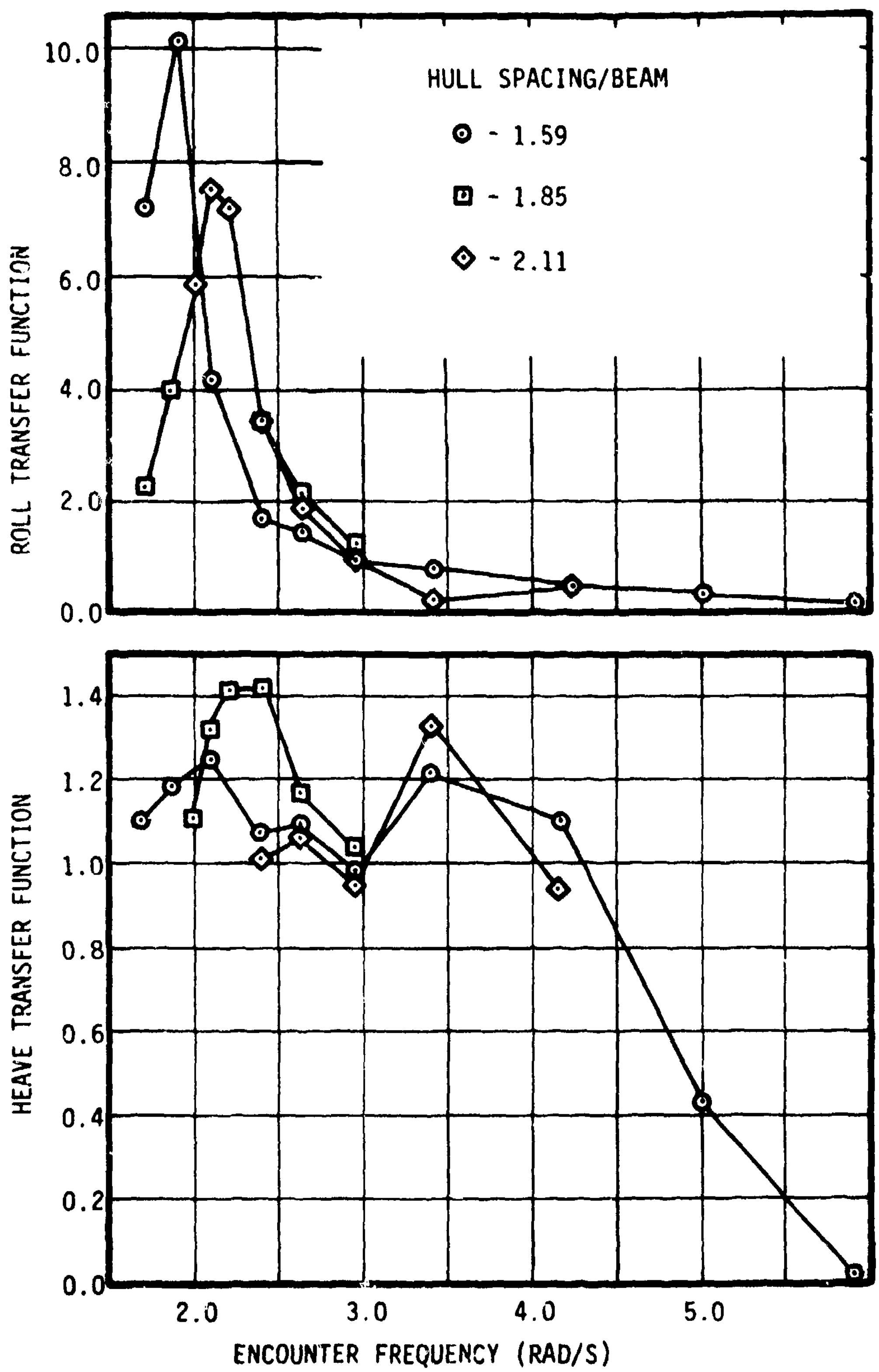


Figure 10 - Transfer Functions of DTNSRDC Model in Beam Seas

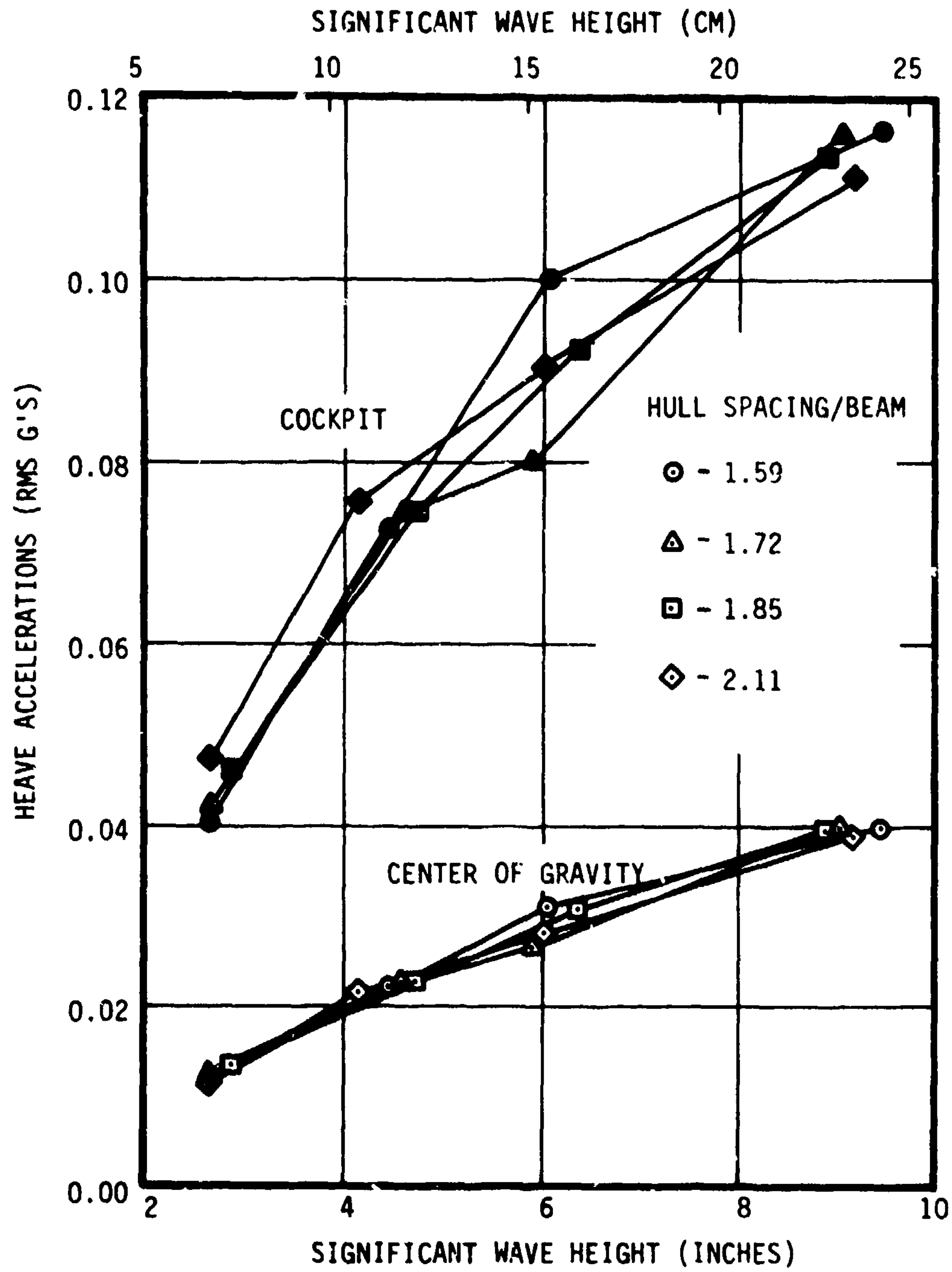


Figure 11 - Heave Accelerations of DTNSRDC Model in Head Seas

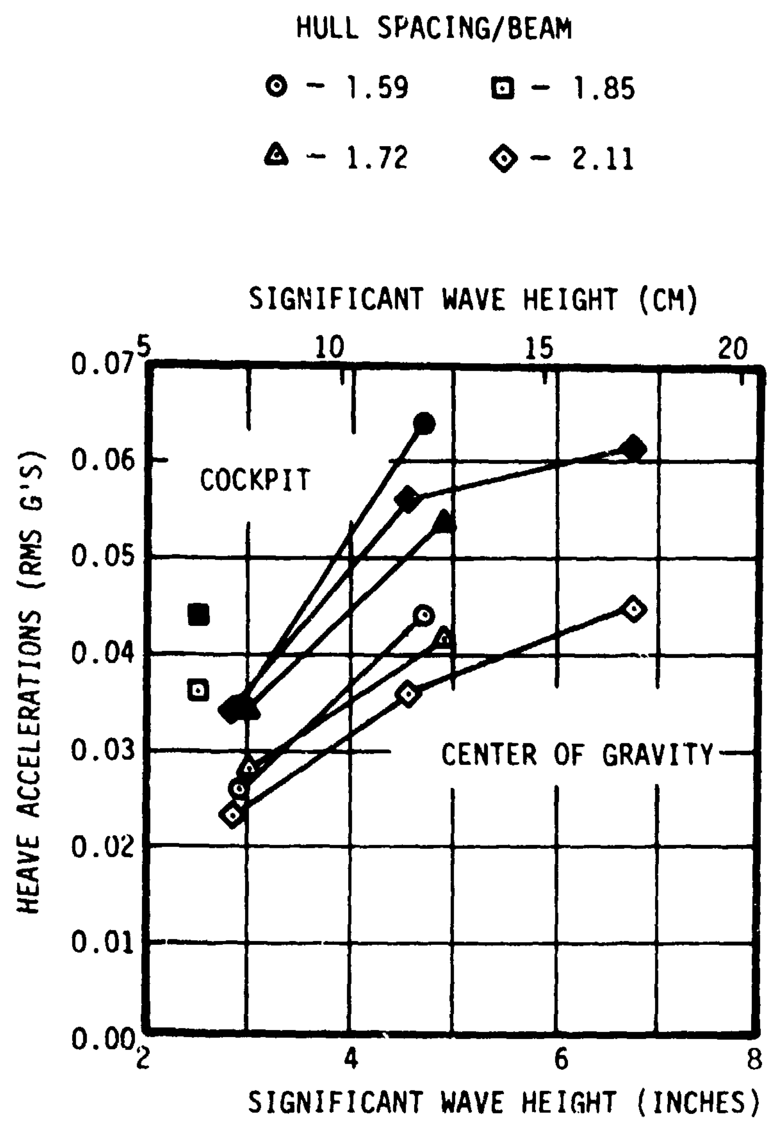


Figure 12 - Heave Accelerations of DTNSRDC Model in Beam Seas

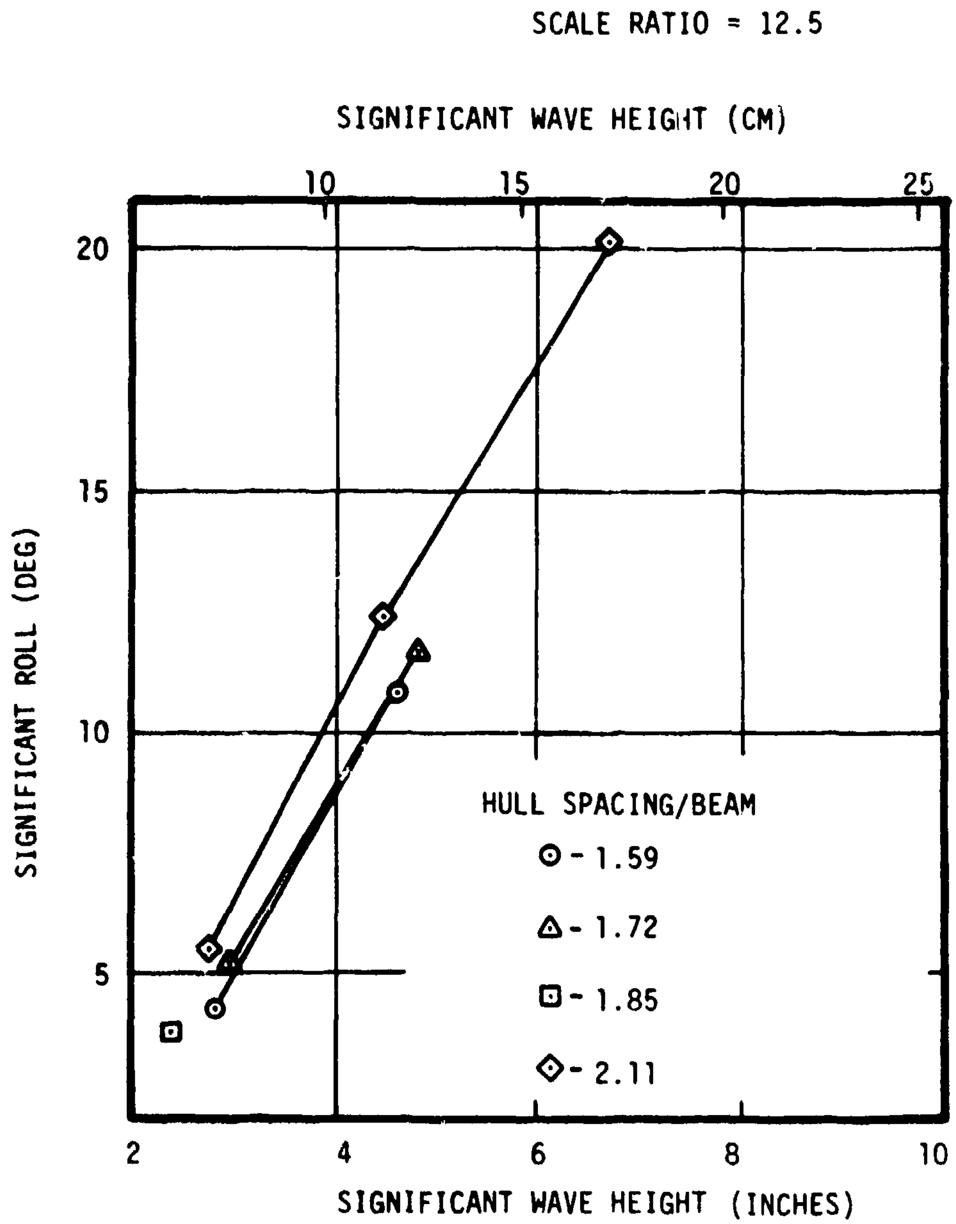


Figure 13 - Roll Displacements of DTNSRDC Model in Beam Seas

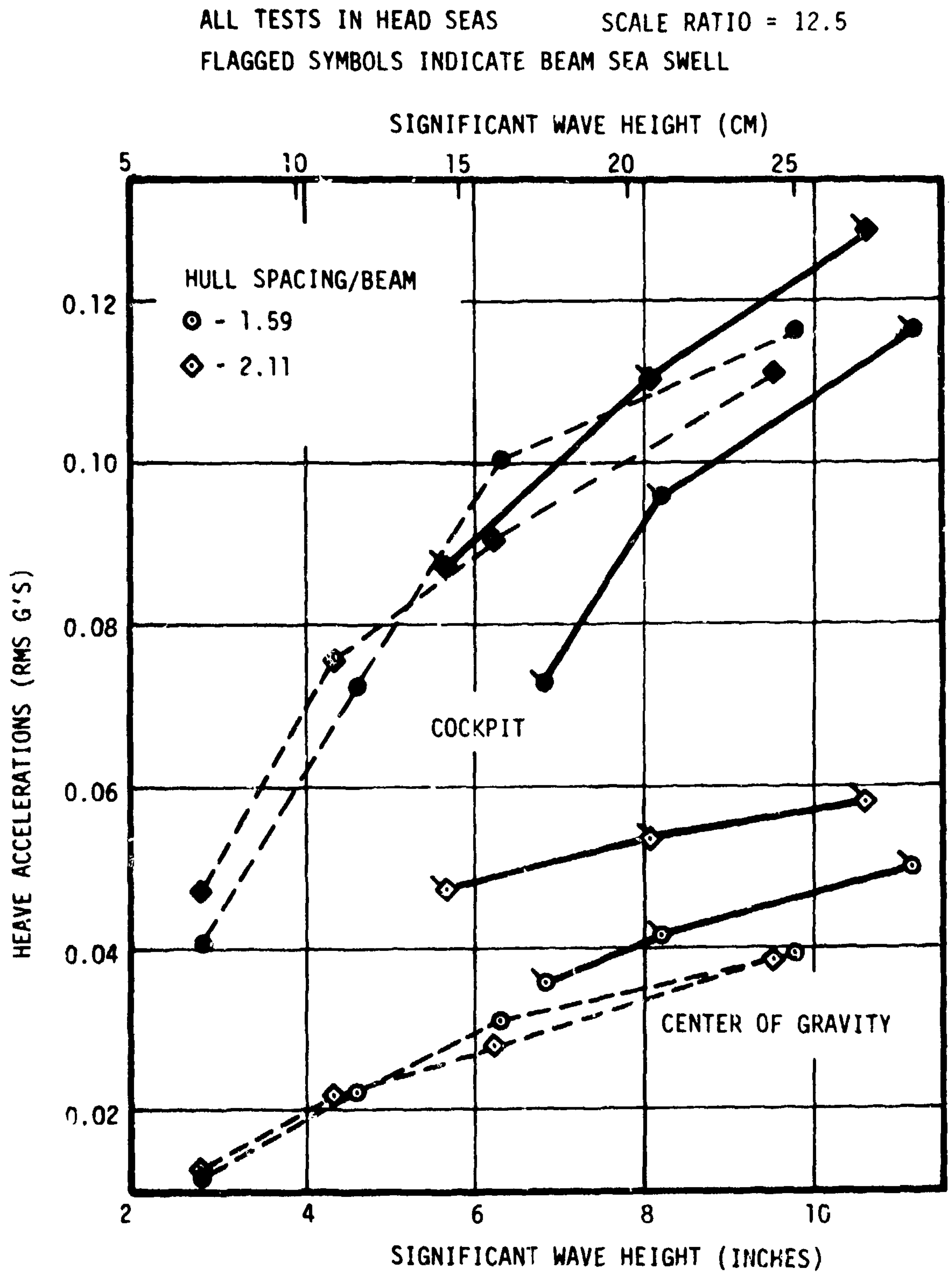


Figure 14 - Heave Accelerations of DTNSRDC Model in Confused Seas

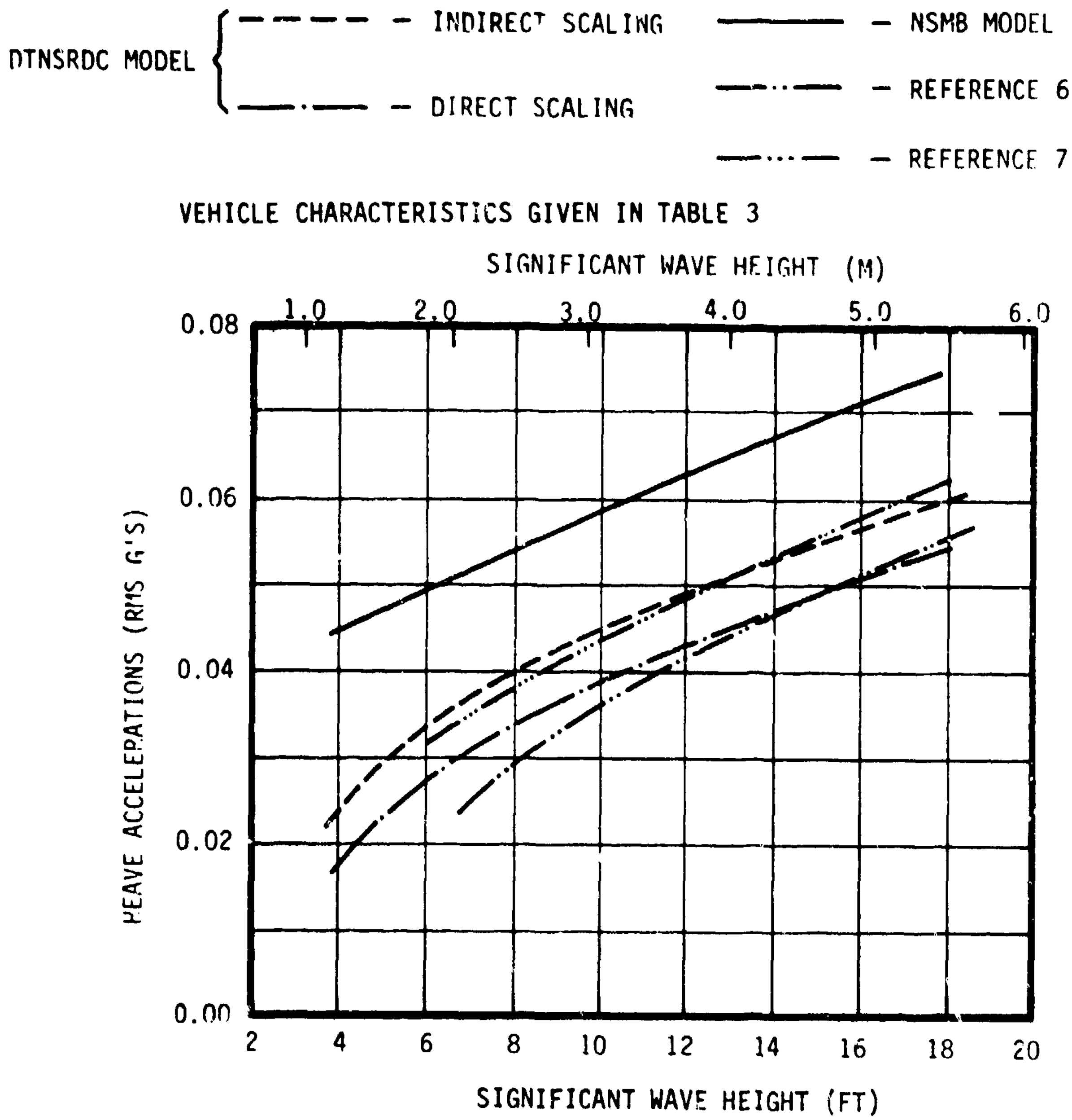


Figure 15 - Heave Accelerations of 1,250,000 Pound (568,000 Kilogram) Aircraft in Head Seas

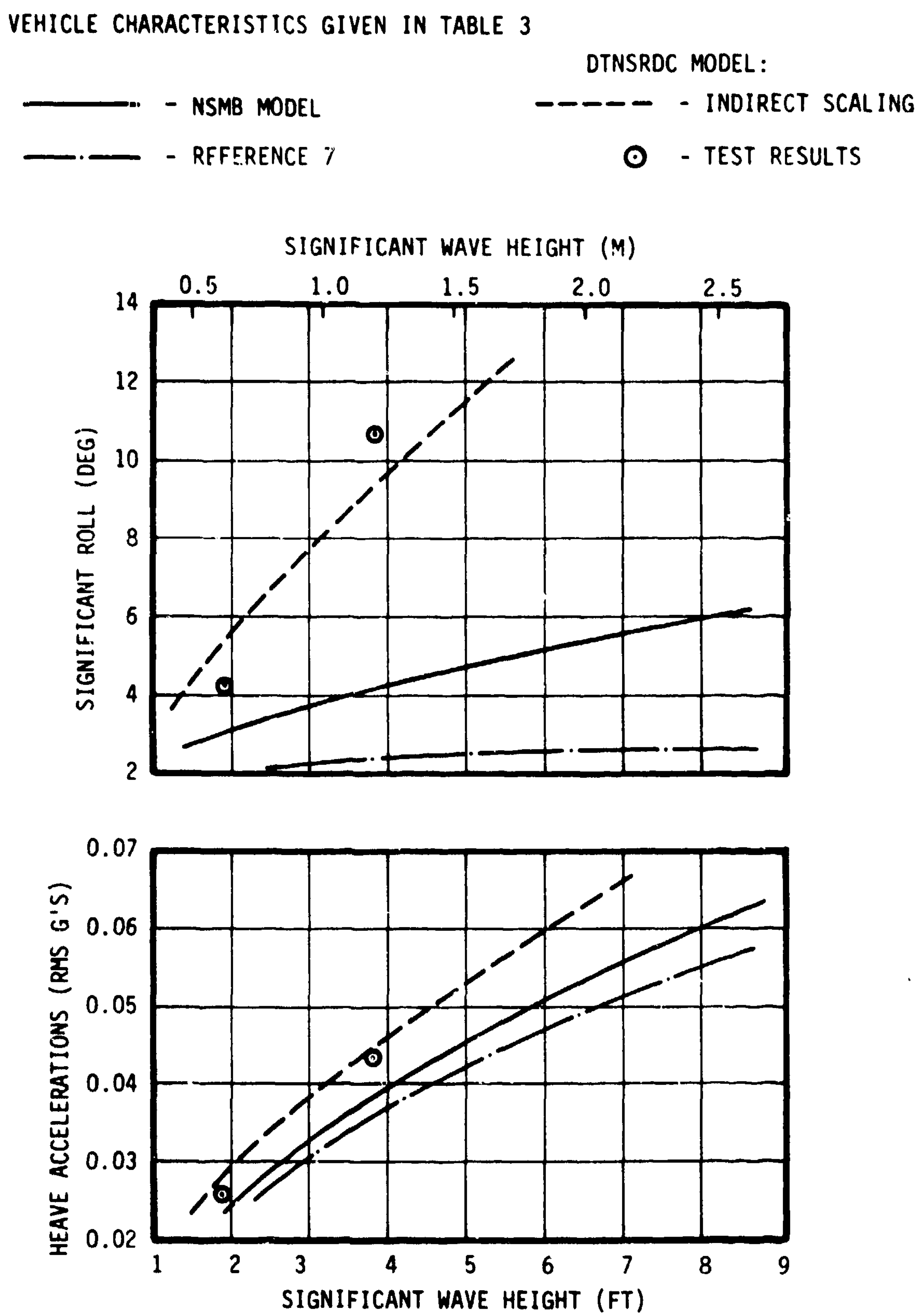


Figure 16 - Motions of 1,250,000 Pound (568,000 Kilogram)

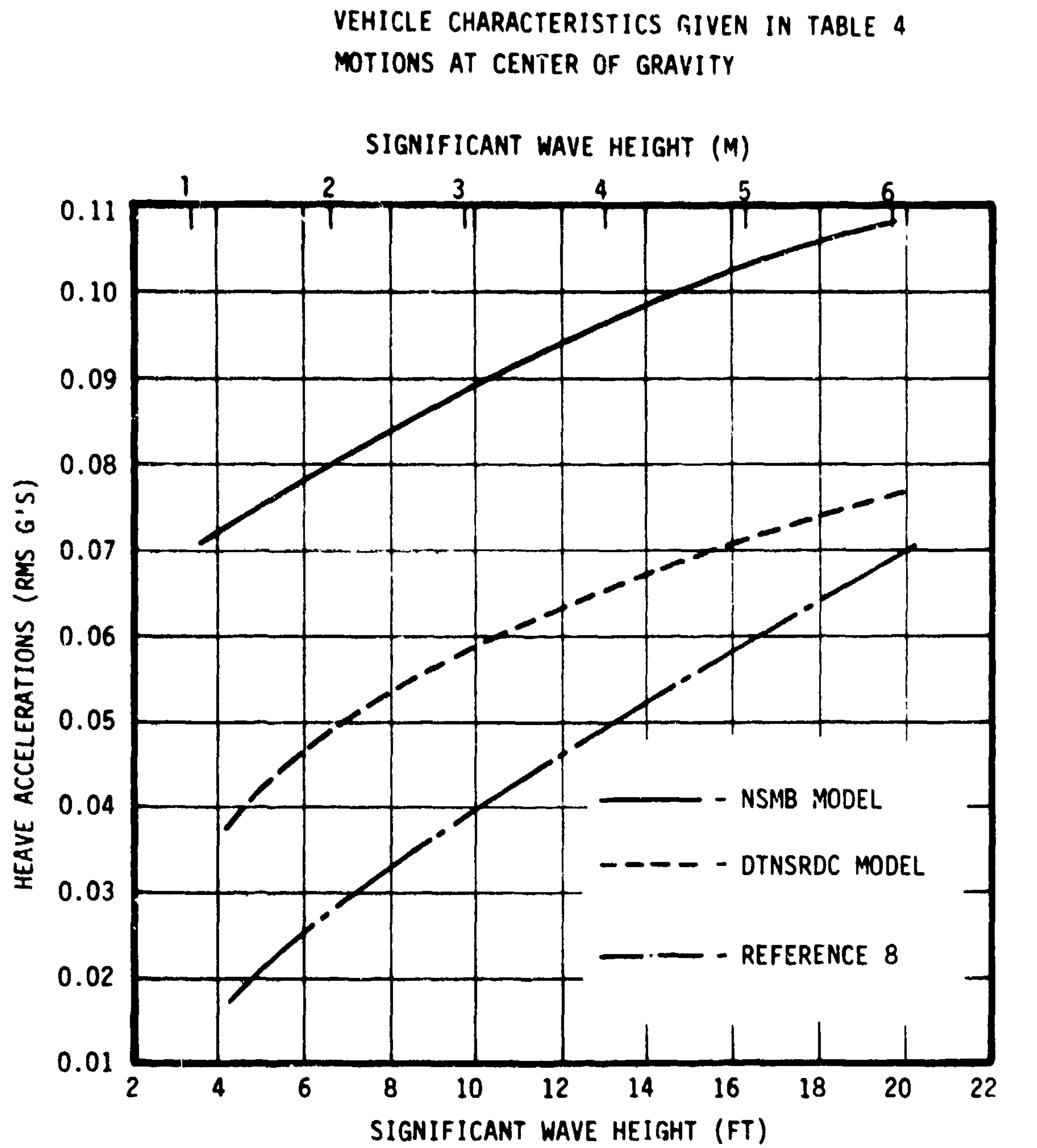


Figure 17 - Heave Accelerations of 640,000 Pound (291,000 Kilogram) Aircraft in Head Seas

VEHICLE CHARACTERISTICS GIVEN IN TABLE 4
MOTIONS AT CENTER OF GRAVITY

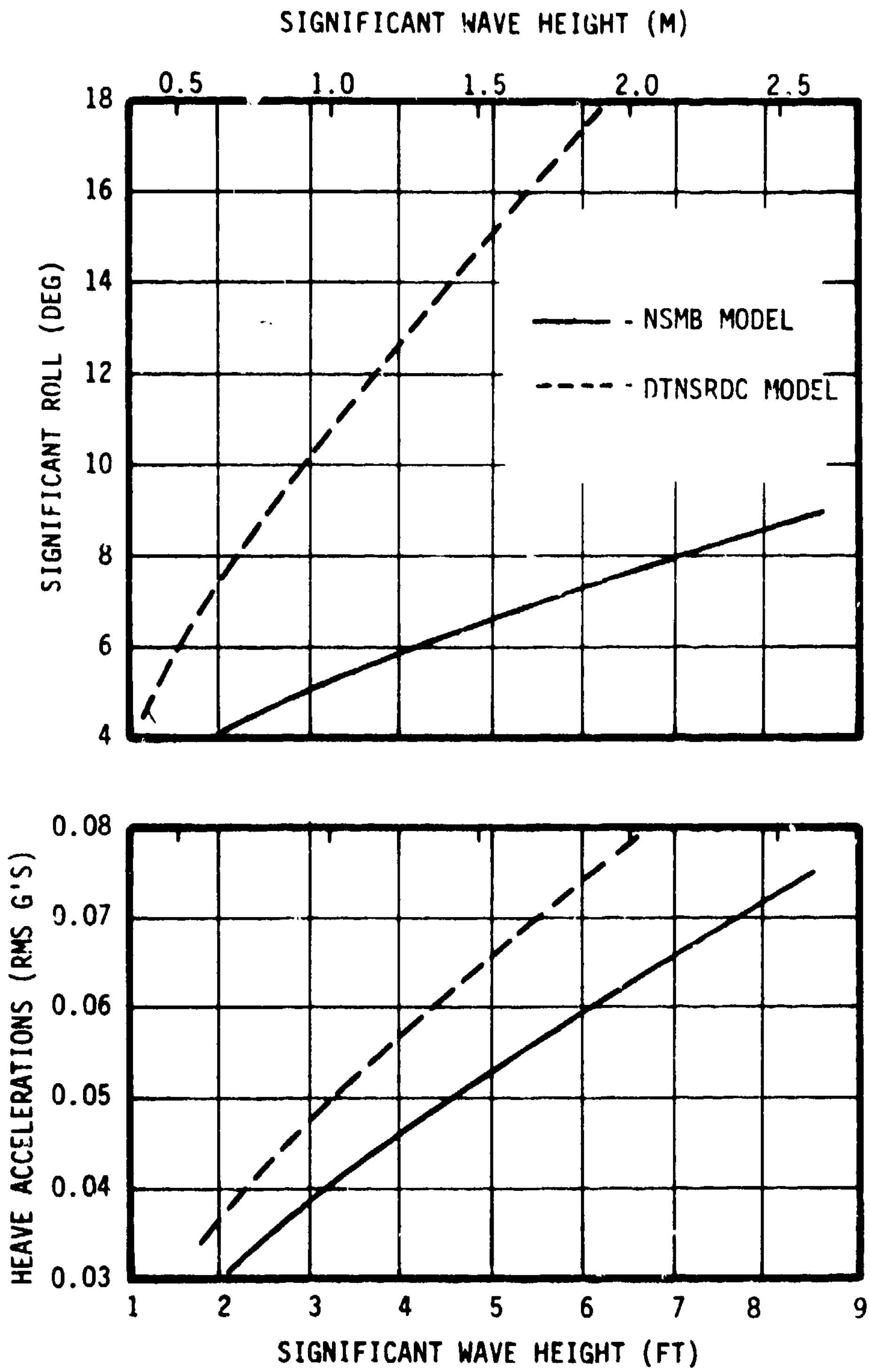


Figure 18 - Motions of 640,000 Pound (291,000 Kilogram)

Aircraft in Beam Seas

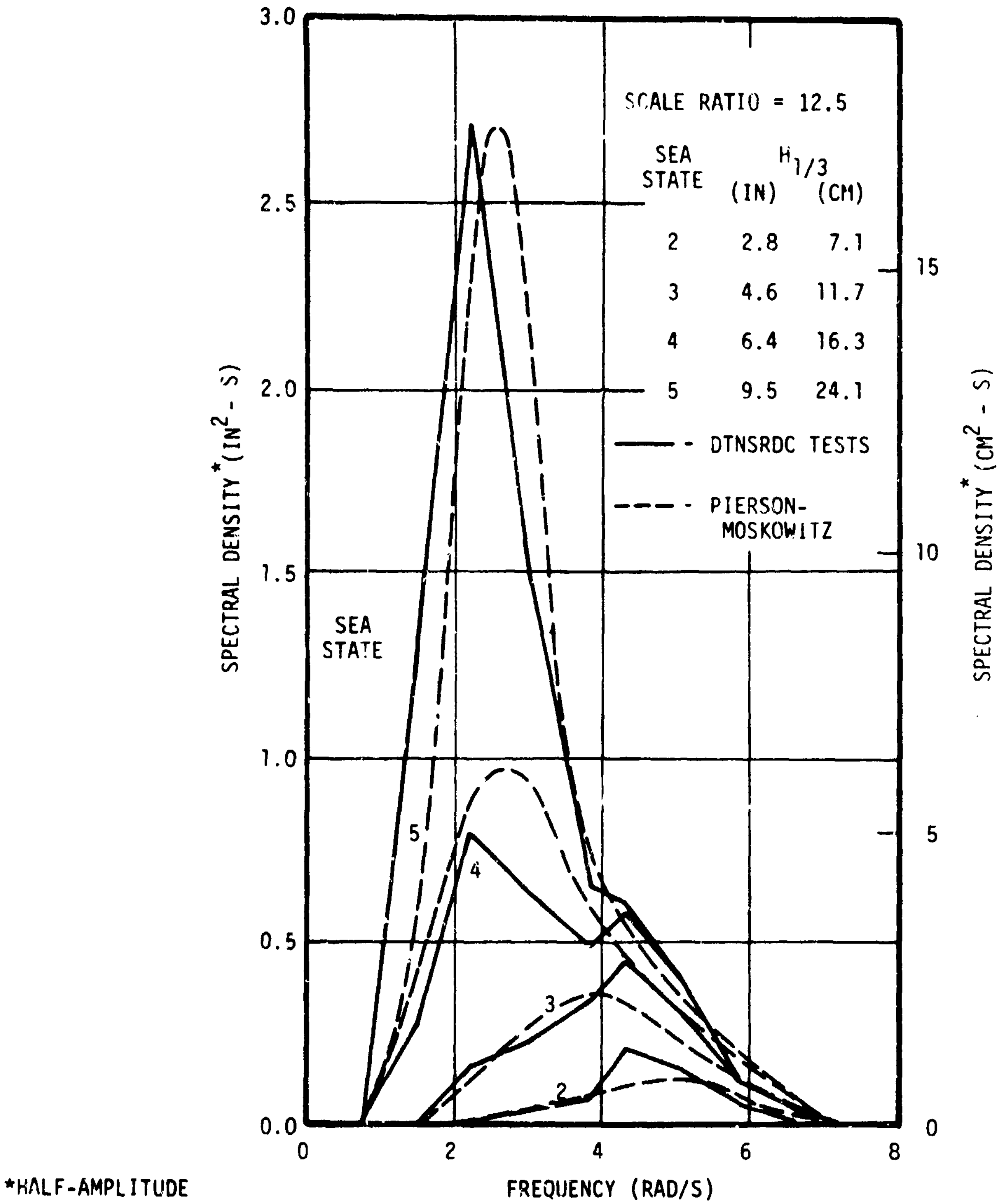


Figure 19 - Sea Spectra Used in DTNSRDC Test Program

TABLE 1 - NSMB MODEL CHARACTERISTICS

| | | |
|---|---|---|
| Displacement | 18.2 lb | (8.26 kg) |
| Waterline Length | 64.2 in. | (163.0 cm) |
| Maximum Waterline Beam | 3.94 in. | (10.0 cm) |
| Wing Span | 94.5 in. | (240.0 cm) |
| Wing Height (above water) | 5.12 in. | (13.0 cm) |
| Pitch Radius of Gyration | 29.1 in. | (74.0 cm) |

| | Roll Radius of Gyration in. (cm) | | |
|---|---|---|---|
| Hull Spacing/Beam | 1.0 | 3.0 | 7.0 |
| CG Height (above keel) | | | |
| 8.82 in. (22.4 cm) | 3.94 (10.0) | 31.5 (80.0) | 70.9 (180) |
| 7.44 in. (18.9 cm) | 7.87 (20.0) | 39.4 (100) | 86.6 (220) |

TABLE 2 - DTNSRDC MODEL CHARACTERISTICS

| | | |
|---|---|---|
| Displacement | 640 | lb (291 kg) |
| Waterline Length | 139 | in. (353 cm) |
| Maximum Waterline Beam | 11.4 | in. (30.0 cm) |
| Wing Span | 228 | in. (570 cm) |
| Wing Height (over water) | 31.2 | in. (79.2 cm) |
| Fuselage Clearance (over water) | 7.80 | in. (19.8 cm) |
| Pitch Radius of Gyration | 44.4 | in. (113 cm) |
| Roll Radius of Gyration* | 34.8 | in. (88.4 cm) |
| CG Height (above keel) | 17.1 | in. (43.4 cm) |

*Roll Radius of Gyration was fixed

TABLE 3 - CHARACTERISTICS OF VARIOUS 1,250,000 POUND (568,000 KILOGRAM) CATAMARAN AIRCRAFT DESIGNS

| | NSMB | DTNSRDC | Reference 6 | Reference 7 |
|---|---|---|---|---|
| **Scale Ratio** | 41.0 | 12.5 | 1.0 | 1.0 |
| **Waterline Length, ft (m)** | 220 (67.1) | 145 (44.2) | 120 (36.6) | 114 (34.8) |
| **Length/Beam (at waterline)** | 16.4 | 12.2 | 10.0 | 9.5 |
| **Beam Loading** | 4.00 | 5.83 | 5.65 | 5.65 |
| **Hull Spacing/Beam** | 2.0 | 1.6 | 2.5 | 2.5 |
| **Wing Span, ft (m)** | 323 (98.3) | 238 (72.4) | 317 (96.7) | 317 (96.7) |
| **Wing Height (above water), ft (m)** | 17.5 (5.34) | 32.5 (9.91) | 32.0 (9.76) | 32.0 (9.76) |
| **Fuselage Clearance (above water), ft (m)** | 17.5 (5.34) | 8.13 (2.48) | 12.0 (3.66) | 12.0 (3.66) |
| **Roll Radius of Gyration, ft (m)** | 60.4 (18.4) | 23.0 (7.00) | 56.2 (17.1) | 38.0 (11.6) |
| **Pitch Radius of Gyration, ft (m)** | 40.1 (12.2) | 46.0 (14.0) | 58.6 (17.9) | 48.1 (14.7) |
| **CG Height (above keel), ft (m)** | 30.1 (9.18) | 17.8 (5.41) | 29.0 (8184) | 32.5 (9.91) |

TABLE 4 - CHARACTERISTICS OF VARIOUS 640,000 POUND (291,000 KILOGRAM)
CATAMARAN AIRCRAFT DESIGNS

| | NSMB | DTNSRDC | Reference 8 |
|---|---|---|---|
| Scale Ratio | 32.8 | 10.0 | 1.0 |
| Waterline Length, ft (m) | 176 (53.6) | 116 (35.3) | 161 (49.1) |
| Length/Beam (at waterline) | 16.4 | 12.2 | 12.5 |
| Beam Loading | 4.00 | 5.83 | 3.80 |
| Hull Spacing/Beam | 2.0 | 1.6 | 1.5 |
| Wing Span, ft (m) | 258 (78.6) | 190 (58.0) | 234 (71.2) |
| Wing Height (above water), ft (m) | 14.0 (4.27) | 26.0 (7.93) | 26.0 (7.93) |
| Fuselage Clearance (above water), ft (m) | 14.0 (4.27) | 6.50 (1.98) | 6.00 (1.83) |
| Roll Radius of Gyration, ft (m) | 48.3 (14.7) | 28.7 (8.75) | 30.3 (9.24) |
| Pitch Radius of Gyration, ft (m) | 32.1 (9.79) | 36.8 (11.2) | 33.2 (10.1) |
| CG Height (above keel), ft (m) | 24.1 (7.34) | 14.2 (4.32) | 39.4 (12.0) |

## REFERENCES


1. Meeks, T. L. and P. J. Mantle, "The Advanced Naval Vehicle Concepts Evaluation," AIAA Paper 76-846, AIAA/SNAME Advanced Marine Vehicles Conference, Arlington, Virginia (Sep 1976).

2. Smethers, R. G., "A Modern Technology, Open-Ocean Seaplane Design," SAE Paper 760922, SAE Aerospace Engineering and Manufacturing Meeting, San Diego, Calif. (Nov 1976).

3. Payne, P. R., "On Quantizing Ride Comfort and Allowable Accelerations," AIAA Paper 76-873, AIAA/SNAME Advanced Marine Vehicles Conference, Arlington, Virginia (Sep 1976).

4. Wahab, R. and W. A. Swaan, "Model Tests with a Catamaran Seaplane in Waves,: Netherlands Ship Model Basin Report 66-086-ZT (Sep 1966).

5. "Principles of Naval Architecture," Edited by J. P. Comstock, Revised Edition, Society of Naval Architects and Marine Engineers, New York (1967), pp. 660-668.

6. "On-Water Motion Relationships Study - Final Report," Columbus Aircraft Division, Rockwell-International Report NR-76H-137 (Jan 1977).

7. Chung, J. S., "Sea-Loiter Aircraft (Large C/STOL) - Motions and Accelerations of Preliminary LCG Configuration," Lockheed Missiles and Space Company Technical Memorandum 5723-76-082 (Nov 1976).

8. "Study of On-Water Motions Relationships of Surface Loiter Aircraft," Columbus Aircraft Division, Rockwell-International Report NR77H-50 (May 1977).

9. Gersten, A., J. Bonilla-Norat, and L. Murray, "Seakeeping Characteristics of a Preliminary Design for a Sea Loiter Aircraft," Report DTNSRDC/SPD-748-02 (Feb 1977).

## APPENDIX

## SEA SPECTRA USED IN DTNSRDC TEST PROGRAM

The DTNSRDC model was tested in four series of random waves. These waves were generated according to a set of standardized wave programs used as input to the wave generators. The wave programs produced waves which approximated Froude-scaled sea energy spectra. The actual spectra used are shown in Figure 19. These spectra modeled full-scaled Sea States 2, 3, 4, and 5. Data from these random wave tests could be directly Froude-scaled.

For numerical predictions, a Pierson-Moskowitz wave spectra model was used to generate the wave characteristics. This spectra is defined by:

$$S(\omega) = \frac{8.385}{\omega^5} \exp\left\{\frac{-33.54}{(H_{1/3})^2\omega^4}\right\} \qquad \text{(A1)}$$

Figure 19 also presents the amplitude spectra based on this equation for the four sea states considered.

The wave slope spectra, for the Pierson-Moskowitz model, was determined from the amplitude spectrum by:

$$\phi_\zeta(\omega) = \frac{\omega^2 z_\zeta(\omega)}{g} \qquad \text{(A2)}$$

where the wave amplitude was computed from $2S(\omega)=z_\zeta(\omega)^2$.

The difference in wave amplitudes between the theoritical spectra and the actual test spectra undoubtedly contributed to some of the differences in the predicted motions computed by the indirect scaling and direct scaling methods. However, since the motions are calculated by <u>integrating</u> the spectra, it is unlikely that the differences in the wave amplitude spectra could have made any significant contribution to the differences in the predicted motions.